AD-E 400007

COPY NO.

CONTRACTOR REPORT ARLCD-CR-77012

THE EFFECTS OF SHIELDED TOTE BINS ON THE SAFE SEPARATION OF 168 POUNDS OF COMPOSITION A-7 EXPLOSIVE

A. B. WENZEL
SOUTHWEST RESEARCH INSTITUTE

RICHARD M. RINDNER
ARRADCOM PROJECT COORDINATOR

SEPTEMBER 1977

US ARMY ARMAMENT RESEARCH AND DEVELOPMENT COMMAND
LARGE CALIBER
WEAPON SYSTEMS LABORATORY
DOVER, NEW JERSEY

The findings in this report are not to be construed as an official Department of the Army position.

DISPOSITION

Destroy this report when no longer needed. Do not return to the originator.

UNCLASSIFIED
SECURITY CLASSIFICATION OF THIS PAGE (When Data Entered)

REPORT DOCUMENTATION PAGE

READ INSTRUCTIONS BEFORE COMPLETING FORM

1. REPORT NUMBER: Contractor Report ARLCD-CR-77012
2. GOVT ACCESSION NO.
3. RECIPIENT'S CATALOG NUMBER

4. TITLE (and Subtitle): THE EFFECTS OF SHIELDED TOTE BINS ON THE SAFE SEPARATION OF 168 POUNDS OF COMPOSITION A-7 EXPLOSIVE

5. TYPE OF REPORT & PERIOD COVERED: Final Report

6. PERFORMING ORG. REPORT NUMBER: SwRI 02-4343

7. AUTHOR(s): A. B. Wenzel, SwRI; R. M. Rindner, ARRADCOM Project Coordinator

8. CONTRACT OR GRANT NUMBER(s): DAAA21-75-C-0324

9. PERFORMING ORGANIZATION NAME AND ADDRESS: Southwest Research Institute, P.O. Drawer 28510, San Antonio, Texas 78284

10. PROGRAM ELEMENT, PROJECT, TASK AREA & WORK UNIT NUMBERS

11. CONTROLLING OFFICE NAME AND ADDRESS: ARRADCOM, LCWSL, Manufacturing Technology Div (DRDAR-LCM-SP), Dover, NJ 07801

12. REPORT DATE: SEPTEMBER 1977

13. NUMBER OF PAGES: 69p.

14. MONITORING AGENCY NAME & ADDRESS (if different from Controlling Office)

15. SECURITY CLASS. (of this report): UNCLASSIFIED

15a. DECLASSIFICATION/DOWNGRADING SCHEDULE

16. DISTRIBUTION STATEMENT (of this Report)

Approved for public release, distribution unlimited.

18. HRLCD; 19. CR-77012;

17. DISTRIBUTION STATEMENT (of the abstract entered in Block 20, if different from Report)

SBIE; HD-E400 007

18. SUPPLEMENTARY NOTES

19. KEY WORDS (Continue on reverse side if necessary and identify by block number)

Tote bins	Composition C-4
Kevlar composite	Conveyor roller
Composition A-7	Separation distance
Composition B	Detonation

20. ABSTRACT (Continue on reverse side if necessary and identify by block number)

This program was carried out to determine the minimum safe separation distance between stainless steel tote bins protected with Kevlar shielding. Each tote bin contained 168 pounds of Comp[illegible] A-7 traveling on a simulated conveyor system within a tunnel or ramp.

Full-scale tests were conducted to determine: (a) the effectiveness of the Kevlar shield, (b) the minimum safe separation distance in a steel-fiberglass tunnel

DD FORM 1 JAN 73 1473 EDITION OF 1 NOV 65 IS OBSOLETE

UNCLASSIFIED
SECURITY CLASSIFICATION OF THIS PAGE (When Data Entered)

92 100

20. (Cont'd)

configuration, (c) the source of detonation and-or propagation, either primary (tote bin) or secondary (conveyor) fragments, or both, (d) the safe separation distance in a wooden-fiberglass tunnel, and (e) the effects of confinement on detonation and-or propagation of acceptors.

The results of this study are briefly summarized as follows: (1) The thickness of Kevlar tested was ineffective in preventing ignition at 130 feet in a steel tunnel configuration. Even though propagation (detonation) did not occur, a fire broke out at this distance. (2) Primary fragments (tote bin) were the most likely source of detonation and-or propagation. (3) No propagation was observed at 130 feet when a wooden-fiberglass structure was used. (4) Blast-focusing due to the presence of the tunnel walls can affect the trajectory of the fragments as well as the flight velocity.

In the Composition B production line at Holston Army Ammunition Plant, interline distances greater than 130 feet between stainless steel tote bins conveying 168 pounds of Composition A-7 are unacceptable because of production requirements and equipment constraints.

The citation in this report of the names of commercial firms or commercially available products or services does not constitute official endorsement or approval of such commercial firms, products, or services by the US Government.

ACKNOWLEDGMENTS

The author is grateful to Mr. William Seals of ARRADCOM for his helpful comments, suggestions, and cooperation during the course of this investigation. Also, the author wishes to acknowledge the following SwRI staff members for their contributions to this program:

- Mr. Luis Garza - Design, fabrication, and procurement of the experimental setup
- Mr. James Kulesz - Performance of the analysis given in the appendix
- Mr. J. W. Gehring - Editing and preparation of the film
- Messrs. A. C. Garcia, Robert Marin, and John F. Weschler for implementing the field experiments.

The cooperation of these individuals and others is greatly appreciated.

TABLE OF CONTENTS

METRIC CONVERSIONS

The following metric conversions, which conform to ASTM Standard E-380-74 Metric Practice Guide, are provided for the reader's convenience.

Page	U. S.	Metric
1,2,4,6,7,9-12,14,16,18,19	165 $\pm$ 3 lb	74.75 kg $\pm$ 1.36 kg
	130 ft	39.62 m
2,20	260 ft	79.25 m
3,4,6,8,9,10	100 ft	30.48 m
3,5	6 ft	1.83 m
3,5	8 ft	2.44 m
	10 ft	3.05 m
3,19	12 ft	3.66 m
3,5	5 ft	1.52 m
3,4,5,7,19	168 lb	76.10 kg
4,8	90 ft	27.43 m
4,6,8,9,10,12,13	110 ft	33.53 m
5,8	0.072 in.	1.83×10^{-3} m
	60 lb	27.18 kg
	24 in.	6.10×10^{-1} m
5,8,10,11,15,18,19	3/8 in.	9.53×10^{-3} m
5,11,12	3/4 in.	1.91×10^{-2} m
5,10	1-1/2 in.	3.81×10^{-2} m
	1/8 in.	3.18×10^{-3} m
5,8,11,13	2 in.	5.08×10^{-2} m
	4 in.	1.02×10^{-1} m
5,11	6 in.	$1 52 \times 10^{-1}$ m
6	4 oz	112 g
	350 ft	106.68 m

Page	U. S.	Metric
7,8	40 ft	12.19 m
8,9	48 ft	14.63 m
8,9,13	80 ft	24.38 m
	60 ft	18.29 m
8,11,13	1 in.	2.54×10^{-2} m
	6900 ft/sec	2103.12 m/sec
9,10,12,13	120 ft	36.58 m
	255 ft	77.72 m
	350 ft	106.68 m
	200 ft	60.96 m
	6620 ft/sec	2017.78 m/sec
9,13,19	6670 ft/sec	2033.02 m/sec
10,13	5200 ft/sec	1584.96 m/sec
	13 in.	3.30×10^{-1} m
11	5 in.	1.27×10^{-1} m
	16 in.	4.06×10^{-1} m
11,12	1/4 in.	6.35×10^{-3} m
	5-1/2 in.	1.40×10^{-1} m
	12 in.	3.05×10^{-1} m
11,13	4-1/2 in.	1.14×10^{-1} m
	3 in.	7.62×10^{-2} m
12	4 ft	1.22 m
	3 ft	9.14×10^{-1} m
13,14	0.5 in.	1.27×10^{-2} m
	11.5 in.	2.92×10^{-1} m
	3440 ft/sec	1048.51 m/sec
	3210 ft/sec	978.41 m/sec
13,14	7670 ft/sec	2337.82 m/sec
	1790 ft/sec	545.59 m/sec
	8 in.	2.03×10^{-1} m
	4020 ft/sec	1225.30 m/sec

Page	U. S.	Metric
13,14	3410 ft/sec	1039.37 m/sec
	15 in.	3.81×10^{-1} m
	5130 ft/sec	1563.62 m/sec
14	6.5 in.	1.65×10^{-1} m
	2670 ft/sec	813.82 m/sec
	382 ft/sec	116.43 m/sec
	2.5 in.	6.35×10^{-2} m

For Tables 1 through 3, multiply the U. S. measurement by the metric conversion to obtain metric values.

22	1 ft	3.05×10^{-1} m
	1 in.	2.54×10^{-2} m
23	1 ft/sec	3.05×10^{-1} m

For Figures 1-11, the following conversions are to be used:

27	24 in.	6.10×10^{-1} m
	18 in.	4.57×10^{-1} m
	15-3/4 in.	4.00×10^{-1} m
	13-1/4 in.	3.34×10^{-1} m
	12 in.	3.05×10^{-1} m
35	120 ft	36.58 m

For the appendix, the following conversions are to be used:

A-1,A-2,A-7	130 ft	39.62 m
A-1,A-7	1.25 ft	3.81×10^{-1} m
A-2,A-3	4 ft	1.22 m
A-2,A-6,A-7	9 ft	2.74 m
A-4	6.0467 ft	1.84 m
A-5	5.9541 ft	1.81 m

Page	U. S.	Metric
A-5	168 lb	76.10 kg
	3.61×10^{9} in/lbf	8.11×10^{8} m/N·m
	14.7 psi	10.13×10^{4} Pa
	223 psi	15.36×10^{5} Pa
	0.123 psi/sec	8.47×10^{2} Pa/sec
	27.7 psi/sec	19.09×10^{4} Pa/sec
A-6	5.9952 ft	1.83 m
	6.0870 ft	1.86 m
	12.0822 ft	3.68 m
	216 psi	14.88×10^{5} Pa
	0.122 psi/sec	8.41×10^{2} Pa/sec
	27.8 psi/sec	19.15×10^{4} Pa/sec
	12 ft	3.66 m
	6220 ft/sec	1895.86 m
A-7	0.625 ft	1.91×10^{-1} m

For Tables A-1 and A-2, multiply the U. S. measurement by the metric conversion to obtain metric values.

A-12	1 lb	2.205 kg
	in^2	6.45×10^{-2} m
	1 in.	2.54×10^{-2} m
	1 ft/sec	3.05×10^{-1} m

SUMMARY

The tests described in this report were performed as part of an overall Safety Engineering Program entitled "Safety Engineering in Support of Ammunition Plants" conducted under the guidance of the Manufacturing Technology Directorate, Picatinny Arsenal, Dover, New Jersey. These tests were a follow-on of a previous test program conducted by Picatinny at the Sierra Army Depot, Herlong, California, to determine a safe separation distance between tote bins containing 165 ± 3 lb of Composition A-7 inclosed in a tunnel structure, simulating existing tunnel or ramp structures connecting operations buildings in a production plant. Present designs and equipment are predicated on transporting the A-7 explosive in stainless steel tote bins covered by plastic lids.

The results of the exploratory program conducted at Sierra indicated that there is no safe spacing between tote bins at a distance of less than 130 ft in a steel-fiber glass tunnel structure. Spacing greater than 130 ft is unacceptable by the production facilities because of production requirements and equipment constraints. A small-scale test program was initiated by Picatinny to come up with a solution for reducing the propagation hazard and thus reduce the required safe spacing. This small-scale program showed that three approaches could be successful. These approaches included the substitution of plastic materials for fabrication of the tote bins, the placement of fragment-stopping shields between tote bins, and the application of energy absorbing materials to the exteriors of the bins themselves. Because of cost, schedule, and ease of implementation, the application of a Kevlar® composite shield to the exterior of the bin was considered to offer the most promise.

Therefore, the program conducted at Southwest Research Institute (SwRI) was designed to generate data to answer the following questions:

- What is the effectiveness of the Kevlar® shielding?
- Can a safe separation distance of 130 ft or less be obtained in a steel tunnel configuration with shielded bins?
- Is the source of detonation and/or propagation to a shielded acceptor bin due to primary (tote bin) or secondary (conveyor) fragments, or both?
- Can a wooden-fiber glass tunnel structure provide safe separation distance between donor and acceptors at 130 ft?
- What effect does the tunnel configuration have on detonation and/or propagation of an acceptor?

The answers to these questions are given in detail in the text of this report and are briefly summarized below:

(1) The thickness of Kevlar® tested was ineffective in preventing ignition at 130 ft in a steel tunnel configuration. Even though propagation (detonation) did not occur, a fire was experienced at this distance.

(2) Primary fragments (tote bin) were the most likely source of detonation and/or propagation.

(3) No propagation was observed at 130 ft when using a wooden-fiber glass structure. However, it was determined that the stiffness and rigidity of the tunnel have an effect on safe separation. Therefore, had the stiffness of the wooden tunnels tested been the same as that existing in a production plant, we suspect distances greater than 130 ft might have been required.

(4) Blast focusing due to the presence of the tunnel walls can affect the trajectory of the fragments as well as flight velocity.

To solve this problem, three alternatives are recommended: (1) fabricate the tote bins of 7075-T6 aluminum; (2) increase the distance from the donor to the tunnel walls; and (3) place two donors and two acceptors side by side and increase the distance between double donors and double acceptors to 260 ft. Further investigation of these alternatives is recommended.

INTRODUCTION

This report describes an experimental program conducted by Southwest Research Institute (SwRI) for the U. S. Army Picatinny Arsenal, Dover, New Jersey, under Contract DAAA21-75-C-0324. The objective of this program was to:

> Determine the minimum safe separation distance (relative to explosion propagation) between stainless steel tote bins protected with Kevlar®* shielding. Each tote bin contained 168 lb of Composition A-7 traveling on a simulated conveyor system within a tunnel or ramp.

To accomplish the above objective, 25 full-scale tests were conducted. The actual test firings were made at a remote site within Camp Bullis, a part of Ft. Sam Houston, near San Antonio, Texas. This program was conducted in support of the Army's Ammunition Plant Modernization Program for the proper design and safe use of conveyor systems to transport bulk high explosives to various production, handling, and packing operations of ammunition plants.

Present designs of the modernized plant in the Composition B line at the Holston Army Ammunition Plant (HAAP) are predicated on transporting the explosive in stainless steel tote bins covered by plastic lids with each bin containing 168 lb of Composition A-7. Current U. S. Army Materiel Command regulation AMCR 385-100 requires that the spacing between stainless steel tote bins on the conveyor be at least 100 ft. This regulation does not mention what effect, if any, the shielding and/or tunnel surrounding the conveyor belt may have on the safe separation distance. The tunnel design presently surrounding the conveyor belts at HAAP consists of a steel framework approximately 6 to 8 ft wide by 10 to 12 ft high by several hundred feet long coupled to a concrete foundation sheathed with fiber glass. The explosive is contained by a stainless steel tote bin and conveyed inside this tunnel by a steel roller conveyor system approximately 5 ft above ground level.

In 1974, a full-scale exploratory test series was undertaken by Picatinny Arsenal at Sierra Army Depot, Herlong, California, in an effort to determine a safe separation distance for the Composition B production line. Twenty-six tests were conducted at Sierra Army Depot.[1] Five tests did not utilize tunnel structures. Twenty tests involved wood-framed, fiber glass-sheathed structures to simulate the plant tunnel or ramp. One test used a steel-framed structure as a simulated tunnel. The results of these tests

---

*Registered trademark of E. I. Du Pont de Nemours & Co., Inc.

[1]W. Seals, R. S. Kukuvka, H. Sarrett, and R. M. Rindner, "Safe Separation Tests of Composition A-7 Explosive in 165-Pound Tote Bins," Tech. Memo No. 2189, Picatinny Arsenal, Dover, New Jersey, October 1975.

showed that detonation and/or propagation was observed up to 90 ft without the confinement of tunnels. Detonation of an acceptor was observed at 100-ft separation with a wooden tunnel. Penetration of an acceptor without detonation occurred at 110 ft with the wooden tunnel structure. When the steel-framed tunnel structure was used, detonation of an acceptor bin was experienced at 130-ft separation.

The major conclusions derived from this program were:

- Stainless steel tote bins containing 168 lb of Composition A-7 may not be spaced at or closer than 130 ft without the risk of propagation of detonation from bin to bin. A safe spacing had not yet been determined.
- Primary (tote bin) and secondary (conveyor) fragments are the most likely agents of explosive propagation.
- Since propagation by fragments is a stoichastic process, definitive conclusions concerning the effect of tunnel confinement could not be drawn.

Because current production and equipment constraints at HAAP limit the separation to more than 130 ft, a series of small-scale tests were conducted at Picatinny Arsenal to find a means of reducing the propagation hazard, thus reducing the required safe spacing.[1] These scaled tests considered the use of Kevlar® and other hard fiber sheets attached to the tote bins, flexible stainless steel mesh suspended between tote bins, and substitution of acrylic type materials for the tote bin material. The results of this small-scale program indicated that all the above techniques appeared to reduce the required safe spacing. However, the report[1] recommended the use of either Kevlar® or NVF hard fiber shields attached to the tote bins as the most promising solution.

Therefore, the tests and analysis reported herein are the results of a set of full-scale tests applying the shielding principles set forth in Reference 1, the results of tests designed to isolate whether primary (tote bin) and/or secondary (conveyor) fragments are the cause of detonation propagation, and last but not least, an effort to explain the effects of the tunnel confinement.

In this report, the experimental setup and instrumentation of the test program conducted by SwRI are given in Section II. The test program, results, and analysis are presented in Section III in the form of tables outlining the complete test data and illustrations. Conclusions and recommendations are made. A 10-minute documentary film was also prepared and submitted to Picatinny Arsenal independently of this report. An appendix describes the analysis used to evaluate the effects of tunnel confinement.

---

[1] *Ibid.*

EXPERIMENTAL PROGRAM

The experimental test layout illustrated in Figure 1 shows one donor charge in the center, with two acceptor charges on either side set at distances D_1 and D_2 from the donor. For the majority of the tests, each donor and acceptor was placed inside a tunnel structure fabricated of steel frames, wooden frames, and/or steel and wooden frames, covered with a liner material made of Masonite® and/or fiber glass to simulate a plant tunnel or ramp. Masonite® was substituted for fiber glass during the exploratory stages of this program because it was substantially cheaper than fiber glass and provided a blast reflective surface which was equal to or stiffer than the fiber glass. Each donor and acceptor consisted of 168 lb of A-7 explosive contained in a stainless steel tote bin. The tote bins used were of the same geometry and size as the containers to be used in the conveyance system at HAAP. Figure 2 illustrates the design of these tote bins. They were fabricated of 0.072-in.-thick, welded type 304 stainless steel sheet. The hinged lids were made of Plexiglas®.

The Composition A-7 explosive used in these tests was manufactured at HAAP and was furnished in cardboard boxes, each containing 60 lb of explosive. Each tote bin was placed on a 5-ft-long steel roller section simulating part of the conveyor system, 5 ft above the floor. The 5-ft distance to the bottom of the tote bin was accomplished by using a 24-in.-diameter Sonotube®. For all tests except one, each tote bin was protected with a sheet of 3/8-in.-thick Kevlar® shielding to reduce the tote bin's vulnerability against primary and secondary fragment impact. In one test only, 3/4-in.-thick Kevlar® was used.

Some tests were made in the open air, and others were made in a tunnel structure. The steel tunnels were fabricated from 1-1/2 in. by 1-1/2 in. by 1/8 in. angle iron. The tunnel sections measured 6 ft in width, 8 ft in height, and 8 ft long.

The wooden frame tunnel structures were constructed of 2-in. by 4-in. lumber to which the sheeting of fiber glass was attached by nailing at every 6 inches. The tunnel sections measured 6 ft in width, 8 ft in height, and 8 ft in length.

All the tests conducted using a tunnel were lined with fiber glass material with the exception of four tests where Masonite® was used instead of fiber glass. The sheathing was applied to the steel tunnel by the use of rivets, normally every 6 inches.

---

*Registered trademark of Masonite Corporation.

†Registered trademark of Rohm and Haas Company.

**Registered trademark of Sonoco Products Company.

Figures 3 and 4 illustrate the setup of a steel tunnel lined with Masonite® and a wooden tunnel lined with fiber glass. The setup illustrated in Figure 3 shows the position of the donor relative to its two acceptors spaced at 100 and 110 ft, respectively. Figure 4 shows only one donor spaced at 130 ft from its acceptor instead of the one donor and two acceptor configurations used in all the tests except this one.

Figure 5 shows a view inside a steel tunnel lined with Masonite®, illustrating the positioning of the stainless steel tote bin, protected with the Kevlar® shield, placed on top of the steel roller system and the Sonotube®.

Initiation of the donors was accomplished by inserting a detonator equivalent to a No. 8 blasting cap into 4 oz of Composition C-4 explosive and placing it into the Composition A-7 explosive in the tote bins. Each test was instrumented with two high-speed framing cameras (Hycams) located in positions C_1 and C_2, as shown in Figure 1, and one real-time slow speed camera located in position C_1. The cameras were located approximately 350 ft from the donor and at an angle of 30° from the tunnel axis.

This level of camera coverage provided documentation of the information shown in Section III of this report. The Hycam high-speed camera settings ranged between 4000 and 5000 frames per second, and the settings for the real-time camera were 60 frames per second. Calculation of fragment velocities was made from the high-speed camera coverage when detonation of the acceptors occurred.

TEST PROGRAM AND RESULTS

Test Program

As mentioned in Section I, the overall objective of this program was to determine the safe separation distance between stainless steel tote bins protected with Kevlar® shielding, containing 168 lb of Composition A-7, traveling on a simulated conveyor system within a tunnel or ramp.

To accomplish this objective, a full-scale test program was designed to generate data that would help answer the following questions:

(1) What is the effectiveness of the Kevlar® shielding?

(2) Can a safe separation distance of 130 ft or less be obtained in a steel tunnel configuration with a shielded bin?

(3) Is the source of detonation and/or propagation to a shielded acceptor bin due to primary or secondary fragments, or both?

(4) Can a wooden-fiber glass tunnel structure provide safe separation distance between donors and acceptors at 130 ft?

(5) What effect does the tunnel configuration have on detonation and/or propagation of an acceptor?

To answer the above questions effectively, a 25-shot test program was planned and conducted. This program consisted of firing

- 3 tests without a tunnel
- 4 tests with a steel-Masonite® tunnel
- 5 tests with a steel-fiber glass tunnel; 2 of these tests substituted the acceptors with a Celotex® filled box to collect the fragments arriving at the acceptor locations.
- 2 tests with one-half of the tunnel made out of steel and the other half made out of wood, both covered with fiber glass
- 11 tests with a wood-fiber glass tunnel

---

*Registered trademark of Celotex Corporation.

The separation of the acceptors relative to the donor was varied from 40 ft to 130 ft.

The open air tests were conducted to answer question (1). The steel tunnel tests were conducted to answer questions (1), (2), (3), and (5). The Celotex® tests were conducted to answer question (3). The wooden tunnel tests were conducted to answer questions (1), (3), (4), and (5).

Results

The results of these tests are summarized in Table 1 and described in more detail below. Table 1 identifies the test program by test number, test material, distance (D_1) from donor to acceptor AC_1, distance (D_2) from donor to acceptor AC_2, the number of impacts that the Kevlar® shielding on acceptors AC_1 and AC_2 received, whether a detonation or burn was experienced by acceptors AC_1 and AC_2, the thickness of the Kevlar® shield used, and the number of penetrations experienced through the shield.

Open Air Tests (No Tunnel)

Test Nos. 2, 3, and 4 were conducted without a tunnel configuration in an effort to determine the effectiveness of the Kevlar® shielding. The separation distance of the acceptors ranged from 40 to 90 ft. A detonation occurred at 48 ft, but none at the other distances. Note from Table 1 that the number of impacts on the Kevlar® shielding ranged between 40 to 45 up to separation distances of 80 ft. The number of impacts at 90 ft ranged between 10 to 15, marking a significant decrease. All the fragments recovered from the shield were stainless steel (tote bin). No steel fragments (conveyor) were recovered from the shields. In Test No. 3, one stainless steel fragment penetrated the shield of AC_1 at 48 ft, denting the tote bin. In Test No. 4, AC_1 at 90 ft remained in an upright position. AC_2 at 60 ft was blown to the ground by the blast. A fragment completely penetrated the Kevlar® shield of AC_1, leaving an approximate 1-in. hole. A thin hole was also located approximately 2 in. above AC_1 tote bin.

Reference 1 reported detonation at 100 ft from a donor without shield and penetration of a bin above the explosive level at 110 ft. In this program, a detonation occurred at 48 ft, with penetration through the Kevlar® and bin at 90 ft, showing that the shield was effective in considerably reducing the separation distance in air. The fragment velocity causing the detonation of the bin in Test No. 2 was calculated from the high-speed film to be 6900 ft/sec.

It must be noted that the velocities calculated from the film were obtained by counting the number of frames from the detonation of the donor until the acceptor detonated. By knowing the distance and the film speed, the velocity is calculated. Remember that before a detonation occurs, the fragment has to penetrate through the 3/8-in.-thick Kevlar® and 0.072 in. of stainless steel. Therefore, the velocity reported is lower than the true velocity because of the time required to penetrate the shield and the bin.

Steel Tunnel Tests

To determine if a safe separation distance of 130 ft or less can be obtained in a steel tunnel configuration, Tests 1, 5, 6, 7, 8, 11, 12, and 13 were conducted. Tests 1, 5, 6, and 7 were conducted using Masonite® as a liner material for the steel frames. Fiber glass lining was used in the other tests reported in this series. The separation distance of the acceptors ranged from 48 to 130 ft. Detonations occurred at 48, 80, 100, and 110 ft, and a complete burn at 130 ft. Note from Table 1 that neither detonations nor burn propagated at 100 and 120 ft. The reasons why no propagation occurred at these distances are twofold: (1) propagation by fragments is a stochastic process, and (2) at this stage in the program, the importance of the method of application of the shielding material to the steel framework was not recognized. Initially, the shielding material was riveted to the steel framework at a random spacing, thereby varying the rigidity of the shielding material and the venting process. By the time Shots 12 and 13 were conducted, the importance of rigidity was recognized, and great care was taken in the application of the shielding material, ensuring that it was installed as rigidly as possible. When this was done, two consecutive burns were experienced at 130 ft. A brief discussion of each test is given below.

Test No. 1

In this test, the steel tunnel was covered with Masonite® material. The separation distance of the acceptors was 80 ft for AC_1 and 48 ft for AC_2 (see Table 1). Roller systems were placed under the donor and acceptors. The donor and both acceptors detonated, and the complete tunnel was destroyed. Figure 6 shows the extent of damage to the tunnel. Pieces of the angle frame were found as far as 255 ft from the side of the tunnel. The camera C_2 shield, located approximately 350 ft from acceptor AC_2, was struck. Extra frame assemblies, located at 200 ft from the end of the tunnel, were pierced. The average terminal velocities of the fragments causing the detonations at AC_1 and AC_2 were measured from the high-speed camera to be 6620 ft/sec and 6670 ft/sec, respectively.

Test No. 5

This test was identical to Test No. 1 except that the distances from donor to acceptors were increased to 100 and 120 ft. Roller systems were placed under donor and acceptors. Only the donor charge detonated, and 6 frames (48 ft) on either side of ground zero were completely destroyed. The subsequent 6 frames on either side of ground zero lost all the Masonite® covering. The lost Masonite® could not be reused, but the remaining frames were reused although they were full of holes. The Kevlar® shield at AC_1 received approximately 20 hits, but none penetrated through the shield. Seven hits were recorded in the Sonotube® supporting AC_1. The shield of AC_2 received approximately 26 impacts. One fragment penetrated through the shield, but did not penetrate the tote bin. Figure 7 shows the damage done to the bin. Approximately 30 impacts were received by the Sonotube® below AC_2. All the fragments recovered from the Kevlar® material were stainless steel.

Test No. 6

This test was identical to Test No. 5. Donor and acceptor AC_2 located at 100 ft detonated. A typical view of damage done to the tunnel is illustrated in Figure 8. Twenty frames were completely destroyed, 7 frames could be recovered, and the remaining were reusable. The Kevlar® shield on AC_1 received approximately 27 hits, but none penetrated the shield. All fragments recovered from the shield were stainless steel.

Test No. 7

This test was identical to Test No. 5 except that the distances from the donor to the acceptor were changed to 110 for AC_1 and 120 ft for AC_2. Donor and acceptor AC_1 detonated. The fragment velocity calculated from the film was 5200 ft/sec. A total of 19 frames were completely destroyed, 8 frames could be recovered, and 6 frames were reusable. The Kevlar® shield of AC_2 received two large hits and approximately 30 small impacts. One of the larger hits went through the Kevlar® and made approximately a 1.5-in.-diameter spherical dent with a fracture approximately 13 in. from the bottom of the tote bin. The other impact made a 3/8-in. depression on the bin with the fragments still imbedded in the back side of the Kevlar®. A closeup view of this impact is given in Figure 9. Approximately 30 hits were recorded in the Sonotube® below AC_2. Figure 10 shows the rear view of the tote bin assembly, showing the number of penetrations into the Sonotube® and also the penetrations into the Masonite® shielding around the steel tunnel at a distance of 120 ft from the donor. All the fragments recovered from the Kevlar® shield were stainless steel.

Test No. 8

This test was identical to Test No. 7 except that fiber glass shielding was used instead of Masonite®. Only the donor charge detonated. Six frames on either side of ground zero were completely destroyed. The subsequent 5 frames on either side of ground zero lost all the fiber glass covering. The remaining frames were reusable, although they were full of holes. The shield of AC_1 received approximately 34 hits, but none penetrated through the thickness of the shield. The shield of AC_2 received approximately 25 impacts, but none penetrated through the Kevlar®. Twelve hits were recorded in the Sonotube® below AC_1, and 7 hits were recorded in the Sonotube® under AC_2. Figures 9 and 10 show closeup views of the damage done to the shield and Sonotube®, respectively, from the fragment impacts.

Test No. 11

This test was a repeat of Test No. 7 except that the acceptors were located at a distance of 130 ft from the donor. Only the donor detonated, and there was no propagation into the acceptors. However, AC_1 was impacted a minimum of 5 times, with one fragment penetrating through the shield at the upper left location. The Sonotube® holding AC_1 was impacted 25 times, and a large piece of steel angle iron was on the ground in front of the base of

the Sonotube.® AC_2 was impacted 9 times, but none of the fragments penetrated the Kevlar.® The Sonotube® under AC_2 was impacted 10 times. All the fragments recovered from the shield were stainless steel. Nine frames were destroyed, 7 frames were uncovered, and the rest were reusable.

Test No. 12

This was a repeat of Test No. 11. AC_1 was hit; fragments penetrated the tote bin and caused it to burn. This burn resulted from a stainless steel fragment which was recovered in the tote bin. This fragment had sufficient energy to perforate the shield, but not to cause a detonation.

The recovered tote bin had two holes. One of the holes was 2 in. by 5 in., located in the upper left corner of the bin where the bin bends; the other was a 3/4-in.-diameter hole located approximately 16 in. from the bottom of the center of the bin where it bends. All the Kevlar® and Sonotube® were consumed in the fire. There was a chunky stainless steel fragment approximately 1/4 in. in diameter inside the tote bin which caused the burn. Inside the bin there were several pieces of stainless steel which appeared to be pieces of melten bin. There was a large piece of angle iron located in front and at the foot of the Sonotube® location. The smaller 3/4-in.-diameter hole was attributed to the chunky stainless steel fragment found inside the bin. There was no apparent evidence of what caused the larger hole in the bin. It is believed that this hole was caused by the impact of an angle iron component which grazed off after impact. There were no small angle iron fragments in the vicinity of the Sonotube.® Visual observations indicated that the bin and Sonotube® remained standing until the fire consumed the Sonotube®, causing it to fall. AC_2 was hit 8 times. Three hits were large, and one penetrated through the Kevlar.® AC_2 Sonotube® was hit 20 times, and all the frames in D_1 were consumed by the fire. Nine frames were completely destroyed. Twenty frames were either consumed by fire or panels blown up. Six frames were reusable.

Test No. 13

This test consisted of detonating a donor charge located 130 ft from the two acceptor charges. The tunnel material on the AC_1 side was steel frame covered with the fiber glass. The tunnel material on the AC_2 side was wood frame covered with fiber glass. The AC_1 side (steel frame) was hit; fragments penetrated the tote bin and caused it to burn. However, the time that it took for the tote bin to catch on fire was about 2 or 3 minutes after detonation of the donor. Note that in Test No. 12 the fire started immediately. In this test, the delay of the burn was probably due to the time that it took the hot fragment to initiate the fire. The AC_1 acceptor was hit 2 times on the left side; the first impact occurred 5-1/2 in. from the bottom of and 1 in. from the left side of the tote bin, making a hole 6 in. long and 1 in. wide. The other hit was 12 in. from the bottom and 2 in. from the left side. The impact made a hole 4-1/2 in. long and 2 in. wide. The third hit was on the right side of the tote bin, 12 in. from the bottom and 3 in. from the right. It made a hole 5-1/2 in. long and 3 in. wide. There were 3 stainless steel fragments found on the ground under the acceptor. Two were

3/4 in. in size, and the third was 1/4 in. in size. The Sonotube® was destroyed in the fire. All fragments penetrating the tote bin were of stainless steel material. There were 5 steel frames destroyed, 3 frames where the panels were blown off, and 11 frames where fire destroyed the fiber glass.

Discussion of Test Results with Composition A-7 Acceptors in Steel Tunnel

(1) The 3/8-in.-thick Kevlar® shield did not provide sufficient protection to have a safe separation distance at 130 ft in a steel tunnel configuration.

(2) The method of installing the fiber glass and/or Masonite® shielding to the steel frames has an effect on the results. It was observed that the more rigid the tunnel structure is made, the more vulnerable the tote bins are to fragmentation impact. A focusing effect due to the presence of the tunnel, which caused propagation of the acceptors, was observed through a comparison of the open air and steel tunnel results.

(3) All the fragments recovered from the Kevlar® shielding were of stainless steel material, indicating that the fragments arriving at the acceptor locations were from the donor tote bin.

To further substantiate these observations, two tests were conducted where the two acceptors were replaced by a box of Celotex® catcher material to capture all the fragments arriving at the acceptor locations. The results of these tests are described in the section below.

Celotex® Tests

To determine if the source of detonation and/or propagation of a shielded acceptor bin is due to primary (tote bin) and/or secondary (conveyor) fragments, two tests were conducted (Tests 9 and 10) where the acceptors were replaced by a Celotex® catcher box 4 ft wide by 4 ft high by 3 ft deep at distances from the donor of 110 and 120 ft. The catcher box was used to analyze the fragments arriving in the vicinity of the acceptors. The basic data extracted from these tests were depth of penetration into the Celotex® (P) in inches and the mass of the fragments (M) in grams. The impact velocity (V) in ft/sec was calculated by using the BRL calibration equations for velocity versus penetration into Celotex® as a function of fragment mass developed by Project THOR.[2] The equation used for calculating impact velocity was:

---

[2] Personal communication with Mrs. Ann Hafer, U.S.A. Ballistic Research Laboratories, Aberdeen Proving Ground, MD, November 20, 1975. Evaluation quoted by Mrs. Hafer from Falcon Research and Development THOR Report No. 50, Baltimore, MD, dated February 23, 1972.

$$V = \frac{872.7\, P^{0.736}}{M^{0.256}}$$

The constants in this equation apply only for spall steel fragments.

The data obtained for each fragment are reported in Tables 2 and 3. Table 2 gives the fragment data for Test Nos. 9 and 10 for a catcher box location of 110 ft from the donor charge. Table 3 gives the data for Tests 9 and 10 for a catcher box location of 120 ft from the donor charge. Those fragments that have an (S) next to the value of mass denote steel fragments; all others are stainless steel. A brief discussion of each test is given below.

Test No. 9

Thirty fragments were recovered at the 110-ft box (AC_1) location. Twenty-six of these were stainless steel material, and the balance of steel. The stainless steel fragments ranged in weight from 0.04 gram to 6.90 grams and penetrated from 0.5 in. to 11.5 in. of Celotex®. The steel fragments ranged in weight from 0.86 gram up to 7.80 grams, with penetration ranging from 0.5 in. to 4.5 in. of Celotex®. The velocity of the most energetic stainless steel fragment was calculated from Eq. (1) to be 3440 ft/sec for a 5.28-gram fragment and 3210 ft/sec for a 6.90-gram fragment, both of which penetrated 11.5 in. of Celotex®. The highest velocity calculated for a 0.23-gram fragment penetrating 11.5 in. of Celotex® was 7670 ft/sec. The velocity of the most energetic steel fragment was calculated at 1790 ft/sec for a 4.60-gram fragment. Twenty-six fragments were recovered at the 120-ft box (AC_2) location; 16 of these were of stainless steel material, and the balance of steel. The stainless steel fragments ranged in weight from 0.22 gram up to 17.96 grams and penetrated from 2.0 in. to 8.0 in. of Celotex®. The steel fragments ranged in weight from 0.15 gram up to 2.52 grams and penetrated from 1.0 in. to 3.0 in. of Celotex®. The calculated velocities of those stainless steel fragments penetrating 8 in. of Celotex® were 4020 ft/sec for a 1.01-gram and 3410 ft/sec for a 1.93-gram fragment. Refer to Tables 2 and 3 for data on individual fragments. Comparing the velocities of the fragments calculated with those measured from the high-speed camera data on Test No. 1 at 80 ft, which was 6670 ft/sec, and velocities of 5200 ft/sec at 110 ft for Test 7 indicated that the values of velocity calculated from the Celotex® penetration are realistic.

Test No. 10

This was a repeat of Test No. 9. Forty fragments were recovered at the 110-ft box location. All the fragments recovered were of stainless steel material. The weights ranged from 0.03 gram up to 9.7 grams and penetrated from 0.5 in. up to 15.0 in. of Celotex®. The calculated velocity of the fragments that penetrated 15 in. of Celotex® was 5130 ft/sec for a mass of 2.4 grams. Fifteen fragments were recovered at the 120-ft box. All of these were of stainless steel. The weights ranged from

0.03 gram up to 25.4 grams and penetrated from 0.5 in. up to 6.5 in. of Celotex®. The calculated velocity of the fragments recovered at the 6.5-in. depth of Celotex® was 2670 ft/sec with a weight of 2.77 grams. The heaviest fragment (25.4 grams) penetrated 2.5 in. of Celotex® and had a calculated velocity of 382 ft/sec.

Based on the results of Tests 9 and 10 and also from the fragments recovered from the Kevlar® panels of previous tests, indications are that the majority of the fragments and the most energetic ones arriving at the acceptor locations are of stainless steel material, originating from the tote bin of the donor. Also, fragment velocities up to 7670 ft/sec were calculated from the mass and depth of penetration of Celotex®.

Wooden Tunnel Tests

To answer the question of whether a wooden-fiber glass tunnel structure can provide safe separation distance between tote bins at 130 ft, a series of 13 tests was conducted where wooden frames lined with fiber glass were used. In the first two tests (Tests 13 and 14), one-half of the tunnel structure (AC_1 side) was made out of steel, while the other half of the line (AC_2 side) was wooden. Tests 15 through 24 consisted of firing one donor and two acceptors at 130-ft separation. Test 25 consisted of firing one donor and one acceptor at 130-ft separation. Reference is made to Table 1 for a consolidated view of the test results. No detonations or burns of the acceptors were experienced during this test series. A brief discussion of each test is given below.

Test No. 13

On the wooden side of the test setup (AC_2 side), the acceptor was hit twice, but the impacts were very small and did not enter the Kevlar®. The Sonotube® was hit 5 times, all very small impacts. There were 5 frames destroyed, 4 frames with the panels blown off, and the rest were reusable.

Test No. 14

On the wooden side of this test, the acceptor was hit 3 times, all very small impacts. The Sonotube® was hit 10 times, all very small hits. Six frames were destroyed, 4 frame panels blown off, and the rest were reusable.

Test No. 15

On the AC_1 side, the acceptor was impacted a minimum of 17 times. Ten of these impacts were very small, and none of the impacts penetrated through the shield. The AC_2 side was hit 7 times; 4 of these impacts were very small, and none of the fragments penetrated the Kevlar®. The Sonotube® on the AC_1 side was hit 12 times, with 4 of these impacts being very large. On the AC_2 side, the Sonotube® was hit 13 times, all hits very small. A total of 15 frames were destroyed; the rest were reusable.

Test No. 16

This was a repeat of Test No. 15. AC_1 was hit 18 times; one of these fragments penetrated through the 3/8-in. Kevlar® but was stopped at the tote bin. The rest of the hits were very small. AC_2 was hit 6 times; none of these impacts penetrated through the shield. All the fragments were very small. Damage to the line was similar to that experienced in Test No. 15.

Test No. 17

This was a repeat of Test No. 15. No detonation or burning of acceptors occurred. AC_1 was hit 3 times; all impacts were very small, and none penetrated the shield. AC_2 was hit one time; this impact was very small and did not penetrate through the Kevlar®. The Sonotube® was penetrated 11 times on the AC_1 side and 13 times on the AC_2 side. Damage to the line was similar to that in Test 15.

Test No. 18

This was a repeat of Test No. 15. No detonation or burning of acceptors occurred. AC_1 was hit 9 times; all impacts were very small, and none penetrated through the Kevlar®. AC_2 was hit 4 times; all impacts were large, but none penetrated through the shield. The Sonotube® was penetrated 7 times on the AC_1 side and 2 times on the AC_2 side. Damage to the line was similar to that experienced in Test No. 15.

Test No. 19

This was a repeat of Test No. 15. No detonation or burning of the acceptor occurred. AC_1 was hit one time; the impact was very large, but did not penetrate the shield. AC_2 was hit 3 times, all impacts very small; none penetrated through the shield. The Sonotube® was penetrated 12 times on the AC_1 side and 18 times on the AC_2 side. Damage to the line was similar to that experienced in Test No. 15.

Test No. 20

This was a repeat of Test No. 15. No detonation or burning of the acceptor occurred. AC_1 was hit 5 times, all impacts small; none penetrated through the shield. AC_2 was hit 8 times, all impacts very small; none penetrated through the shield. The Sonotube® was penetrated 6 times on the AC_1 side and 7 times on the AC_2 side. Damage to the line was similar to that experienced in Test No. 15.

Test No. 21

This is a repeat of Test No. 15. No detonation or burning of the acceptors occurred. AC_1 was impacted a minimum of 8 times. All the impacts were very small, and none of them penetrated through the shield. On the AC_2 side, the acceptor was hit 12 times, all very small. The Sonotube® on the AC_1 side was penetrated on the AC_1 side 10 times and 8 times on the AC_2 side. A total of 17 frames were destroyed; the rest were reusable.

Test No. 22

This was a repeat of Test No. 15. No detonation or burning of the acceptors occurred. AC_1 was hit 8 times, all very small impacts not penetrating through the shield. AC_2 was hit 6 times; none of the impacts penetrated through the shield. The Sonotube® on the AC_1 side was penetrated 10 times and on the AC_2 side, 13 times. Damage to the line was similar to that exr enced in Test No. 21.

Test No. 23

This is a repeat of Test No. 15. No detonation or burning of the acceptor occurred. AC_1 was hit 6 times, all very small; none of the impacts penetrated the shield. AC_2 was hit 13 times. Eleven of these impacts were very small; however, 2 were fairly large, of the size of a quarter, and both were at the top of the Kevlar® on the right hand side. None of the impacts penetrated through the shield. The Sonotube® on the AC_1 side was penetrated 8 times and on the AC_2 side, 4 times. Damage to the line was similar to that in Test No. 21.

Test No. 24

This was a repeat of Test No. 15. No detonation or burning of the acceptors occurred. AC_1 was hit 4 times; 2 of these impacts were very small, and 2 were very large (the size of a quarter). None of the impacts penetrated the shield. AC_2 was hit 3 times, all very small impacts. The Sonotube® on the AC_1 side was hit 9 times and on the AC_2 side, 7 times. Damage to the line was similar to that experienced in Test No. 21.

Test No. 25

In these tests, only one donor and one acceptor were used at a separation of 130 ft. No detonation or burning of the acceptor occurred. The acceptor was hit 5 times; 3 of these impacts were very small, and 2 were fairly large (the size of a quarter). None of the impacts penetrated the shield. The Sonotube® was hit 8 times, all very small. Damage to the line was similar to that experienced in the wooden side of Test Nos. 13 and 14. Figure 11 illustrates the type of damage experienced by the single wooden line.

Discussion of Results with Wooden Frame Tunnels

The results of these tests showed that at a distance of 130 ft, no propagation or burning of the acceptors was experienced using the wooden tunnel structure. However, comparing the effects of open air with the steel-framed and the wooden-framed tests, it is evident that the rigidity and stiffness of the tunnel have an effect on the safe separation distance. Care must be taken in interpreting the results of these tests because the rigidity and stiffness of the tunnels tes ed here are not typical of those present in actual production plants. Therefore, if we had tested a wooden-framed tunnel with the rigidity of those present in a production plant, we suspect, based on the results of the steel tunnel tests, that separation distances greater than 130 ft would have been required.

On this subject, the reader is encouraged to refer to the appendix of this report for an analytical approach to the effects of the tunnel confinement. This analysis should eventually be applied to a real-life tunnel design, but for this report, the analysis clearly shows that a fragment can be focused into a "hit" trajectory. Depending on the number and energy of these focused fragments, the statistical probability of detonation propagation is enhanced by the tunnel confinement.

Effects of Tunnel Confinement Surrounding a Tote Bin Conveyor Line

Two phenomena have been demonstrated by this program:

- All of the fragments which struck the acceptor line were of stainless steel--therefore, they emanated from the donor tote bin and not from the tunnel support frames or wall material.

- The minimum distances at which propagation occurred were far greater for the confined tests (i.e., with tunnels) than for the unconfined tests (i.e., open air--no tunnel).

It was apparent then that the tunnel did have a significant contributory effect on the propagation, not by contributing to the fragmentation, but rather by focusing the shock wave and/or focusing more fragments into striking the acceptor tote bin.

To examine the feasibility of this "focusing concept," an analysis was carried out to calculate: (1) the peak pressure and impulse of a shock wave after being reflected off the walls of the tunnel; and (2) the interaction of these reflected waves with a fragment in terms of increasing the fragment velocity and in the possibility of redirecting (focusing) a fragment such that a "near miss" fragment would become a "hit" on the acceptor tote bin.

These calculations are shown in detail in the appendix. A variety of sample fragments which had been recovered in the Celotex® tests were weighed, and their presented area and drag coefficient were determined. Four random mass fragments (0.014 to 1.17 grams) were then used as typical cases, and each of these fragments was found to be seriously affected by the reflected shock. Two of the four sample fragments, which had been on a "near miss" trajectory traveling down the tunnel, would have been focused by the shock and redirected into a "hit" trajectory.

The consequences of this focusing effect are now obvious. The confinement offered by the tunnel is significant and must be considered when determining any "minimum safe separation distance." The calculations shown in the appendix merely verify the principle of the focusing effect, but also it is important in the future to consider the real magnitude of the confinement (i.e., steel versus wood framing and the wall material, thickness, mounting ridigity, etc.). Although the analysis performed to date did not consider this effect, the experiments have indicated that the steel-framed tunnel

offered more confinement than did the wood-framed tunnel. In retrospect, an examination of the wood-framed and steel-framed tunnels used in the experiments showed that, although the wall material was identical, it was simply "nailed" to the wood frames, while it was "riveted" to the steel frames. Thus, the rigidity of the reflecting wall surfaces was quite different. Also, the wood offered faster venting, hence falling apart faster than the steel frames.

Summary

From the results of this test program, the answers to the questions asked at the beginning of the section are:

(1) Comparing the results given in Reference 1, where tests in open air were conducted without shields, with the results of this program, the Kevlar® shield was effective in reducing the separation distance. However, applying 3/8-in.-thick Kevlar® for the steel tunnel case was not effective in preventing a fire at 130 ft.

(2) As mentioned above, a safe separation distance greater than 130 ft is required in a steel tunnel configuration.

(3) The primary source of propagation of the acceptors is due to fragments emanating from the donor bin.

(4) At 130-ft separation between donor and acceptor, no propagations or detonations occurred in the wooden tunnel configuration tested by Picatinny and SwRI. However, it was observed that the rigidity and stiffness of the tunnel have an effect on the safe separation distance. Therefore, if a test in a wooden frame tunnel had the rigidity of those present in a production plant, we suspect, based on the results of the steel tunnel tests and the analysis reported in the appendix, that separation distances greater than 130 ft would be required.

(5) The experimental results indicated that the tunnel has an effect on the safe separation distance. The analysis reported in the appendix demonstrated that blast focusing can affect the trajectory of the fragments, and also it is possible to increase the fragment flight velocity when reflective surfaces are present in the vicinity of the donor.

CONCLUSIONS AND RECOMMENDATIONS

Conclusions

(1) Stainless steel tote bins protected with 3/8-in.-thick Kevlar® and containing 168 lb of Composition A-7 may not be spaced at/or closer than 130 ft in a steel tunnel configuration without the risk of propagation and/or detonation from bin to bin. An acceptable solution for spacings of 130 ft or less has not yet been determined.

(2) The primary source of propagation of the acceptors is due to the stainless steel fragments emanating from the donor bin.

(3) At 130-ft separation, no propagation was experienced in the wooden tunnel configuration. However, the test results showed that the rigidity and stiffness of the tunnel have an effect on the safe separation distance. Therefore, if a test in a wooden-framed tunnel has the rigidity of those present in a production plant, we suspect, based on the analysis reported in the appendix and the test results, that separation distances greater than 130 ft will be required.

(4) Blast-focusing can affect the trajectory of the fragments and also increase the fragment flight velocity when reflective surfaces are present in the vicinity of the donor.

(5) Fragment velocities of up to 6670 ft/sec were measured with the high-speed cameras.

Recommendations

Based on the above conclusions, the following changes should be considered:

(1) A simple change which can be made without affecting production schedule or costs is to convey double tote bins (i.e., two bins side by side) and increase their separation distance to 260 ft.

(2) To minimize the primary fragment hazard, the tote bin material must be changed to a material which is compatible with the explosive, meets the safety criteria, has good wear resistant properties, and is brittle. A good selection which meets all the mentioned constraints is an aluminum alloy such as 7075-T6 or 2024-T4.

(3) To minimize blast focusing effects, it is recommended that the tunnel dimension be increased to allow distance to attenuate the blast waves before they reflect from the tunnel walls. A recommended dimension is 12 ft wide by 12 ft high.

These three changes are relatively simple, but offer a high probability of success. Therefore, it is recommended that exploratory tests be conducted to determine the effectiveness of these changes.

Shot No.	Tunnel Material	D_1	D_2	No. of Impacts on AC_1	No. of Impacts on AC_1	Detonation AC_1	Detonation AC_2	Thickness of Kevlar[c] (in.)	No. of Penetrations Through Kevlar[d]
1	S + M	80	48	--	--	DET	DET	3/8	-
2	Air	80	48	45	--	No	DET	3/8	-
3	Air	48	40	40	40	No	No	3/8	1
4	Air	90	60	10	15	No	No	3/8	1
5	S + M	120	100	20	26	No	No	3/8	1
6	S + M	120	100	27	--	No	DET	3/8	2
7	S + M	110	120	--	30	DET	No	3/8	2
8	S + F	110	120	34	25	No	No	3/4	2
9	S + F	120	110	30	26	Celotex[e]	Celotex[e]	---	-
10	S + F	120	110	40	15	Celotex[e]	Celotex[e]	---	-
11	S + F	130	130	5	9	No	No	3/8	1
12	S + F	130	130	--	8	Burn	No	3/8	2
13	S + F W + F	130	130	--	2	Burn	No	3/8	2
14	S + F W + F	130	130	15	3	No	No	3/8	-
15	W + F	130	130	17	7	No	No	3/8	-
16	W + F	130	130	18	6	No	No	3/8	1
17	W + F	130	130	3	1	No	No	3/8	-
18	W + F	130	130	9	4	No	No	3/8	-
19	W + F	130	130	1	3	No	No	3/8	-
20	W + F	130	130	5	8	No	No	3/8	-
21	W + F	130	130	8	12	No	No	3/8	-
22	W + F	130	130	8	5	No	No	3/8	-
23	W + F	130	130	6	13	No	No	3/8	-
24	W + F	130	130	4	3	No	No	3/8	-
25	W + F	130	130	5	--	No	--	3/8	-

NOTES:

S + M = steel-Masonite[b]

S + F = steel-fiber glass

W + F = wood-fiber glass

Distances measured edge-to-edge of bins

Table 1

Results of test program

Shot No.	Tunnel Material	D_1	D_2	No. of Impacts on AC_1	No. of Impacts on AC_1	Detonation AC_1	Detonation AC_2	Thickness of Kevlar[a] (in.)	No. of Penetrations Through Kevlar[a]
1	S + M	80	48	--	--	DET	DET	3/8	-
2	Air	80	48	45	--	No	DET	3/8	-
3	Air	48	40	40	40	No	No	3/8	1
4	Air	90	60	10	15	No	No	3/8	1
5	S + M	120	100	20	26	No	No	3/8	1
6	S + M	120	100	27	--	No	DET	3/8	2
7	S + M	110	120	--	34	DET	No	3/8	2
8	S + F	110	120	34	25	No	No	3/4	2
9	S + F	120	110	30	26	Celotex[b]	Celotex[b]	---	-
10	S + F	120	110	40	15	Celotex[b]	Celotex[b]	---	-
11	S + F	130	130	5	9	No	No	3/8	1
12	S + F	130	130	--	8	Burn	No	3/8	2
13	S + F W + F	130	130	--	2	Burn	No	3/8	2
14	S + F W + F	130	130	15	3	No	No	3/8	-
15	W + F	130	130	17	7	No	No	3/8	-
16	W + F	130	130	18	6	No	No	3/8	1
17	W + F	130	130	3	1	No	No	3/8	-
18	W + F	130	130	9	4	No	No	3/8	-
19	W + F	130	130	1	3	No	No	3/8	-
20	W + F	130	130	5	8	No	No	3/8	-
21	W + F	130	130	8	12	No	No	3/8	-
22	W + F	130	130	8	5	No	No	3/8	-
23	W + F	130	130	6	13	No	No	3/8	-
24	W + F	130	130	4	3	No	No	3/8	-
25	W + F	130	130	5	--	No	--	3/8	-

NOTES:

S + M = steel-Masonite[a]

S + F = steel-fiber glass

W + F = wood-fiber glass

Distances measured edge-to-edge of bins

Table 2

Fragment data at 110 ft

Test 9			Test 10		Test 9			Test 10	
P in.	M grams	V ft/sec	M grams	V ft/sec	P in.	M grams	V ft/sec	M grams	V ft/sec
0.5	0.20	791	0.03	1280	5.5	0.25	4360	0.62	3460
0.5	0.85	546	0.05	1130	5.5	--	--	0.62	3460
0.5	0.86(S) [a]	545	0.08	1000	5.5	--	--	2.31	2470
0.5	--	--	0.30	713	6.0	0.45	4000	0.62	3690
1.0	--	--	0.08	1660	6.0	1.85	2790	2.30	2640
1.0	--	--	0.18	1350	6.0	--	--	2.60	2560
1.0	--	--	0.27	1220	6.0	--	--	2.90	2490
1.0	--	--	0.30	1190	6.0	--	--	9.73	1820
1.5	0.33	1560	0.16	1880	6.5	2.99	2620	5.60	2230
1.5	7.80(S)	696	0.16	1880	7.0	0.22	5380	--	--
1.5	--	--	0.47	1430	7.0	1.54	3270	--	--
1.5	--	--	0.56	1360	7.5	2.21	3140	0.58	4420
2.0	--	--	0.09	2690	8.0	5.33	2630	1.44	3670
2.0	--	--	0.24	2090	8.5	1.23	4000	--	--
2.5	5.72(S)	1100	0.06	3520	8.5	2.26	3420	--	--
2.5	--	--	0.81	1810	8.5	3.04	3170	--	--
2.5	--	--	0.95	1740	9.0	1.09	4300	--	--
3.0	--	--	0.19	3000	9.5	1.74	3970	1.25	4320
3.0	--	--	0.70	2150	10.5	1.56	4400	--	--
4.0	0.04	5510	0.33	3210	11.0	5.49	3300	--	--
4.0	0.05	5210	0.59	2770	11.5	0.23	7670	0.85	5490
4.0	2.09	2010	0.81	2560	11.5	5.28	3440	--	--
4.0	--	--	1.14	2340	11.5	6.90	3210	--	--
4.5	0.09	4890	0.29	3620	13.5	--	--	0.87	6140
4.5	0.43	3280	0.98	2650	15.0	--	--	2.39	5130
4.5	4.60(S)	1790	--	--					

[a] (S) refers to steel fragments; all others are stainless steel.

Table 3

Fragment data at 120 ft

	Test 9		Test 10	
P in.	M grams	V ft/sec	M grams	V ft/sec
0.5	--	--	1.05	518
1.0	0.22(S)[a]	1290	0.03	2140
1.0	0.41(S)	1100	0.28	1210
1.0	--	--	0.38	1120
1.0	--	--	10.45	479
1.0	--	--	25.38	382
1.5	0.19(S)	1800	0.12	2020
2.0	0.29	1990	0.52	1720
2.0	0.42(S)	1810	--	--
2.0	0.43(S)	1800	--	--
2.0	0.50(S)	1740	--	--
2.5	0.15(S)	2780	1.39	1570
2.5	0.52	2020	17.76	821
2.5	0.55(S)	2000	--	--
2.5	3.34	1260	--	--
3.0	0.95(S)	1990	--	--
3.0	2.52(S)	1550	--	--
3.0	2.92	1490	--	--
3.5	1.10	2140	0.64	2460
3.5	1.15	2120	--	--
4.0	2.43	1930	0.65	2700
4.5	1.37	2440	--	--
4.5	1.53	2370	--	--
5.0	--	--	2.49	2260
5.5	2.16	2510	2.32	2470
6.0	1.05	3220	--	--
6.0	17.96	1560	--	--
6.5	--	--	2.77	2670
7.5	1.78	3320	--	--
8.0	1.01	4020	--	--
8.0	1.93	3410	--	--

[a](S) refers to steel fragments; all others are stainless steel.

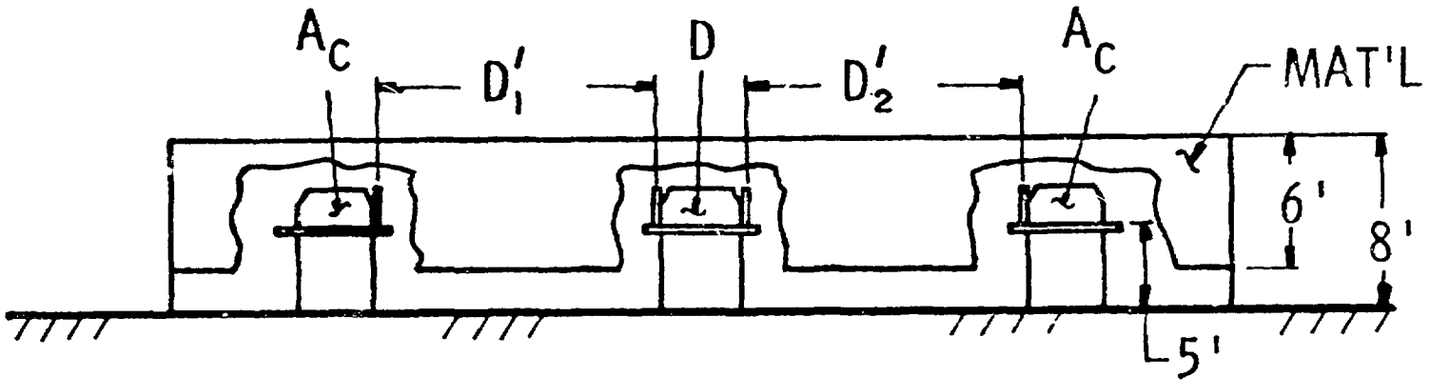

Front view

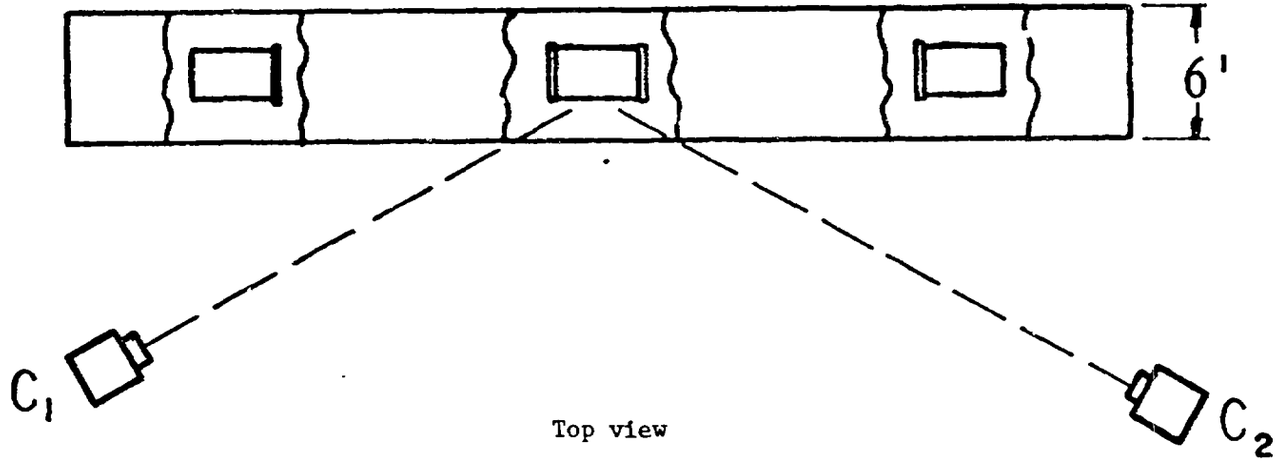

Top view

Fig. 1 Experimental test setup.

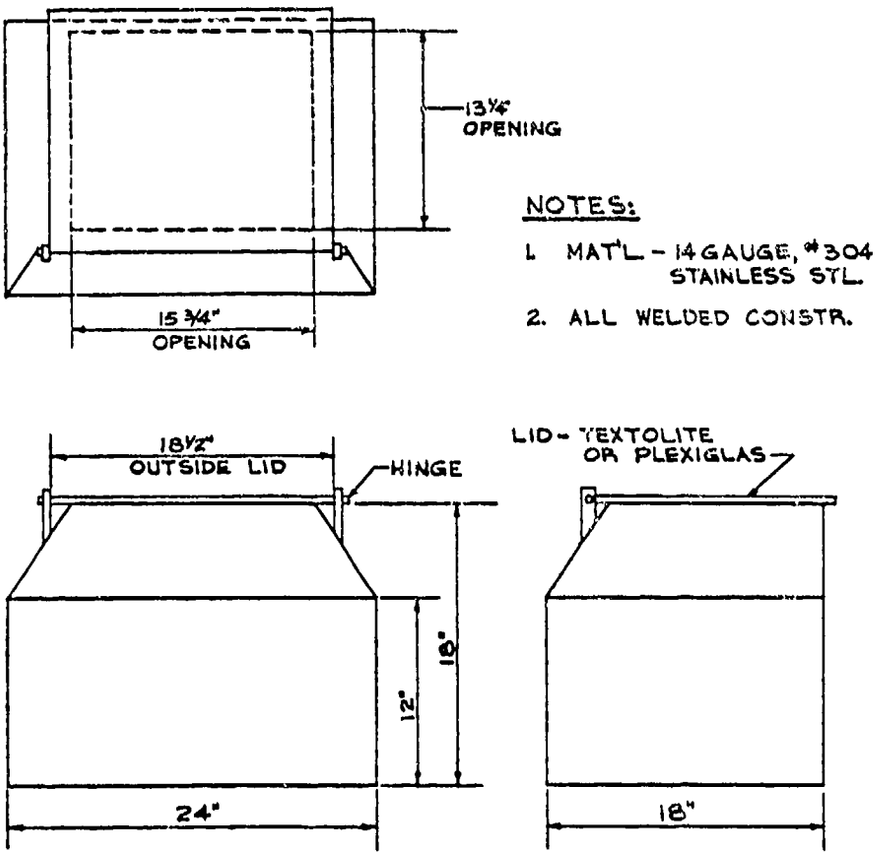

Fig. 2 Tote bin geometry.

Fig. 3 Overall view of test setup using steel Masonite® tunnel.

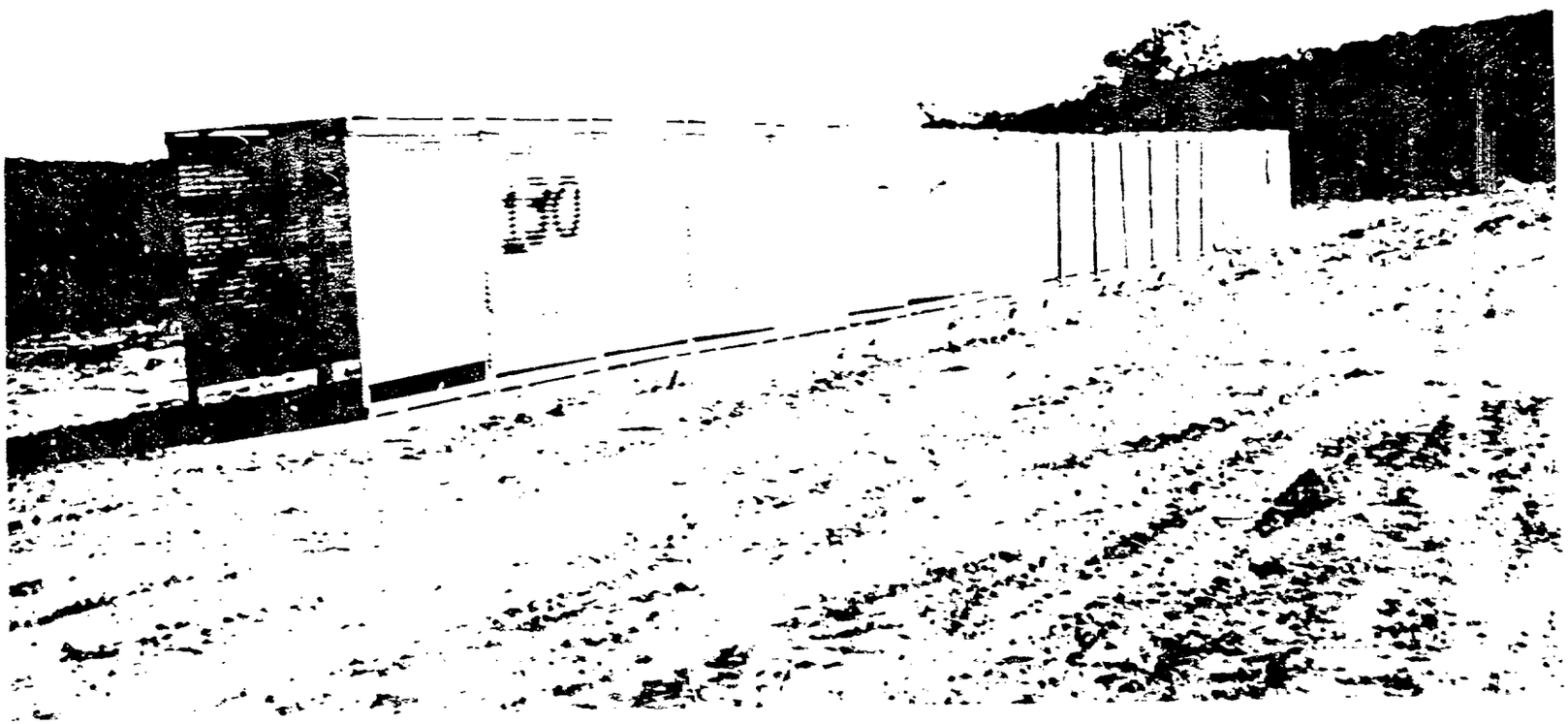

Fig. 4 Overall view of test setup using wood-fiber glass tunnel.

Fig. 5 Inside view of steel-Masonite® tunnel showing donor and acceptor.

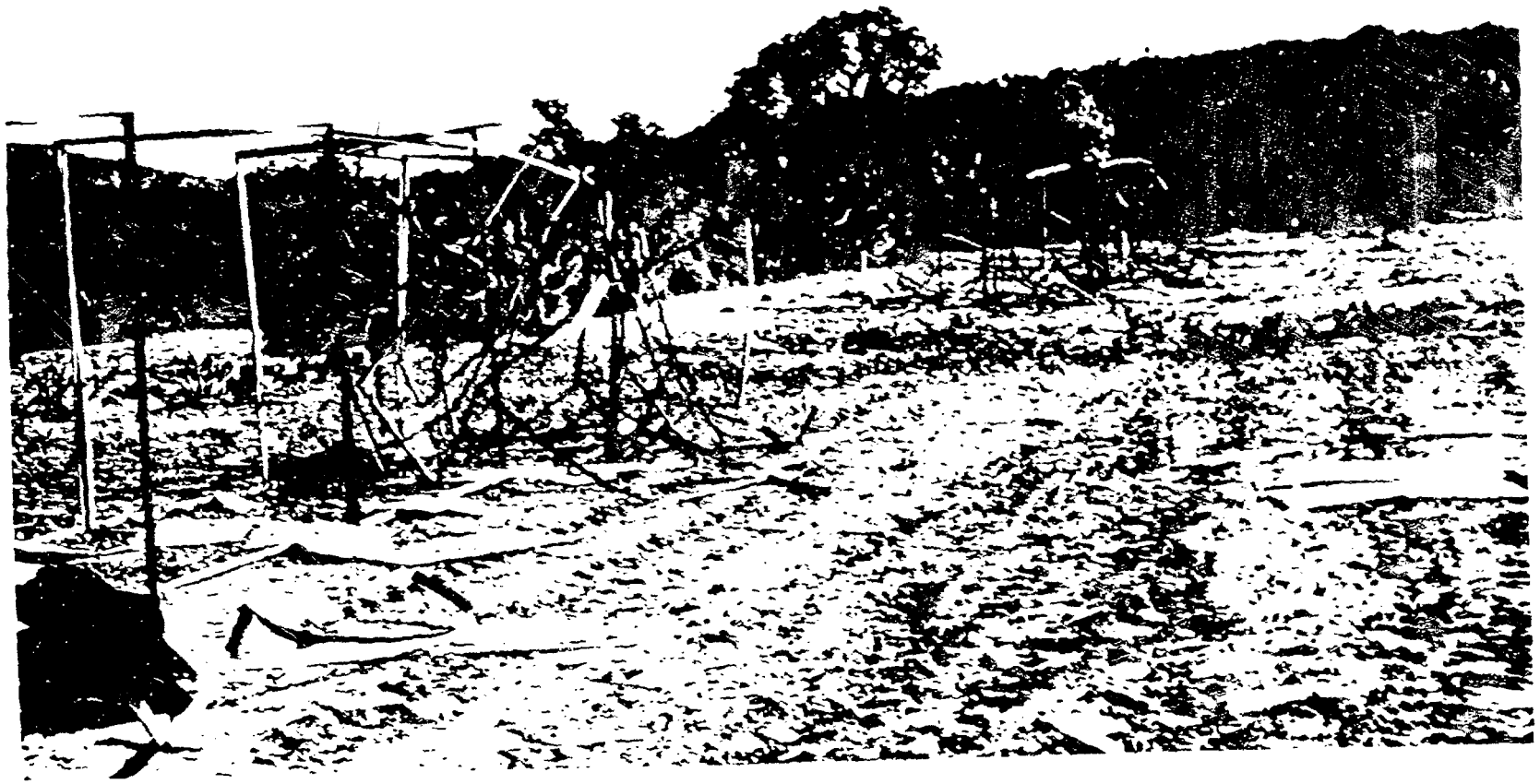

Fig. 6 Destroyed steel tunnel (test no. 1).

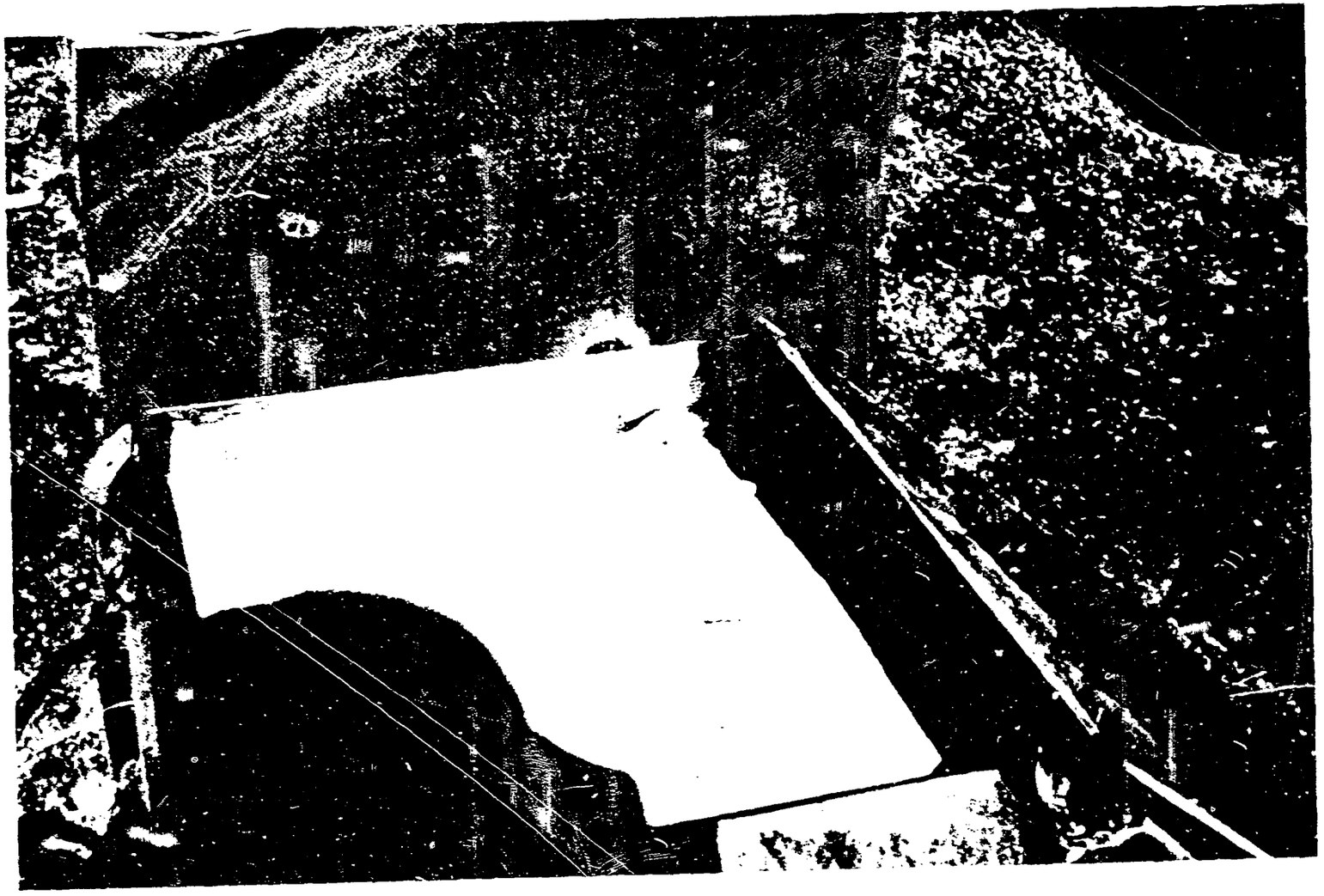

Fig. 7 Impact damage to bin from fragment after penetrating shield (test no. 5).

Fig. 8 Damage to steel tunnel (test no. 6).

Fig. 9 Closeup view of large impacts on Kevlar® shield (test no. 7).

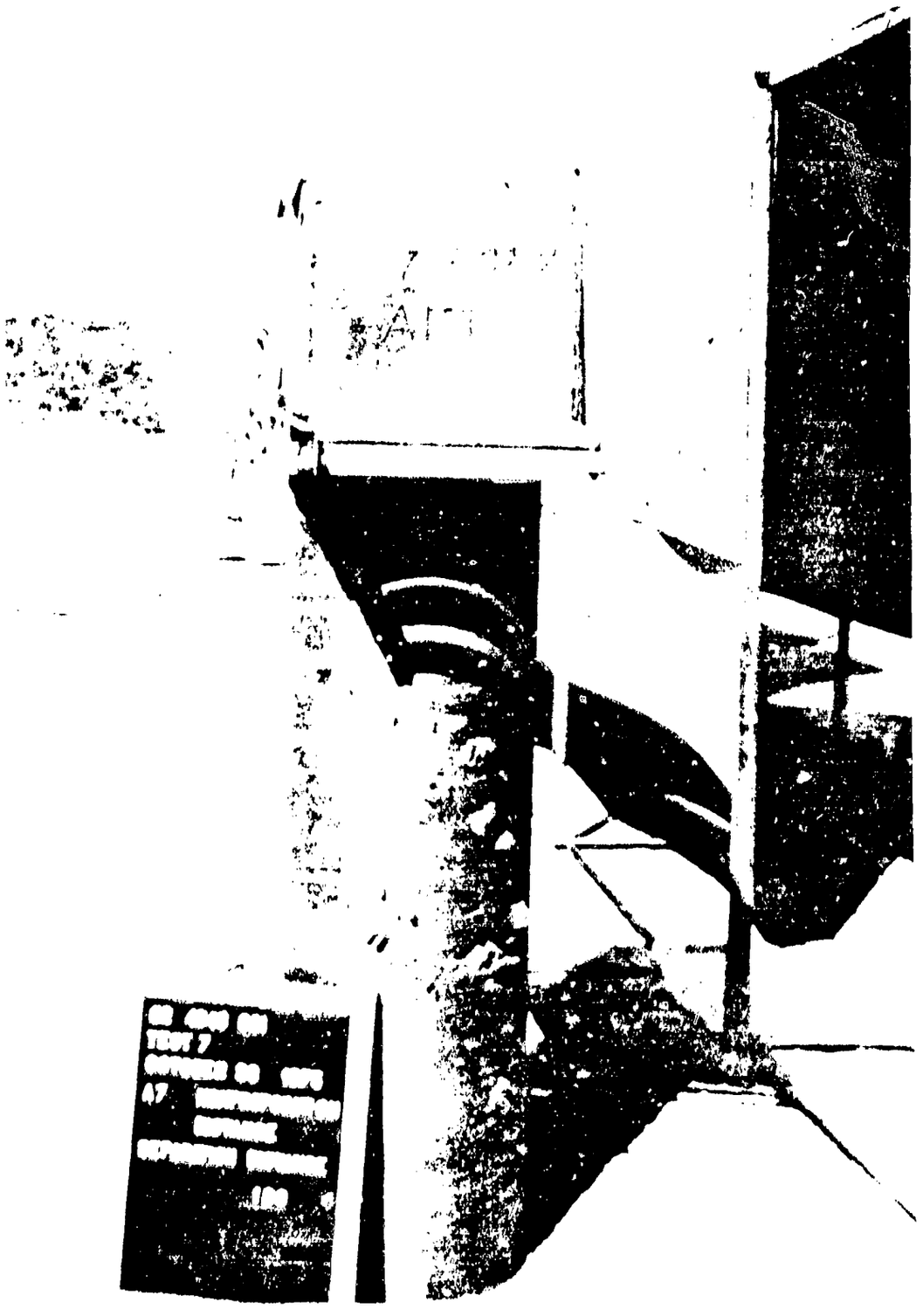

Fig. 10 Closeup view of fragment penetration through Sonotube® and Masonite® shield at 120 ft.

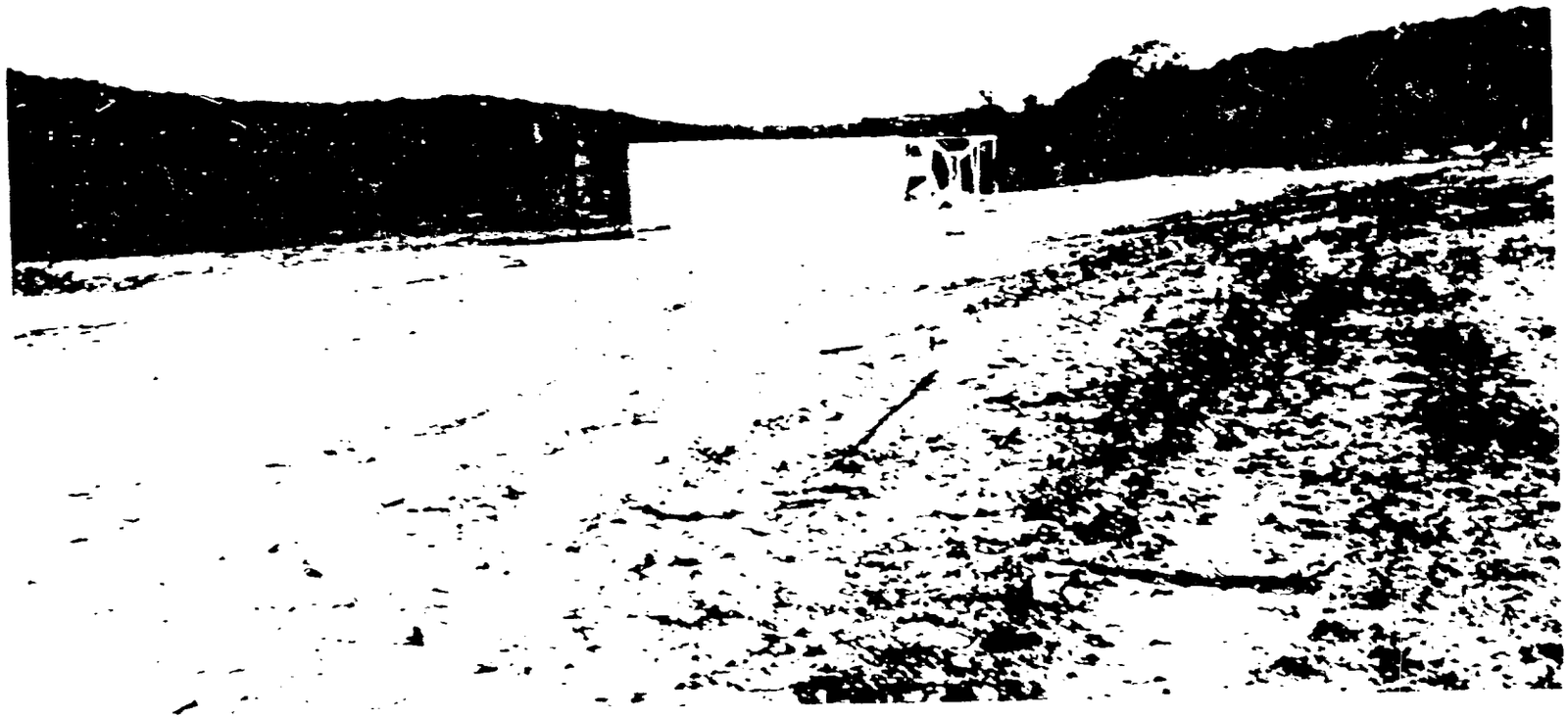

Fig. 11 Damage done to a wooden tunnel (shot no. 25).

APPENDIX

Feasibility of altering trajectory of fragment through interaction with reflected blast waves

Several simplifying assumptions were made in examining the interaction of blast waves with fragments. The main assumptions were:

(1) The angle of incidence equals the angle of reflectance for shock waves.

(2) Incident pressure and impulse are determined by total wave path as if no reflections are present (i.e., no loss of energy in reflection).

(3) The fragment interacts with shock waves from two opposite walls, and the net effect of interaction with reflected shock waves from other walls is zero.

(4) The two shock waves interact with the fragment at the same time.

For this particular problem, we assume that the acceptor is 130 ft from the donor and has a presented edge length of 1.25 ft as shown in Figure A-1. If there are no tunnels present and fragments travel in a straight path, all fragments within the divergence angle δ_0 should strike the acceptor. Thus, if e is the target edge length in feet, and d is distance of the acceptor from the donor in feet, then

$$\delta_0 = 2 \tan^{-1} \left(\frac{e/2}{d} \right) = 0.55° \qquad \text{(A-1)}$$

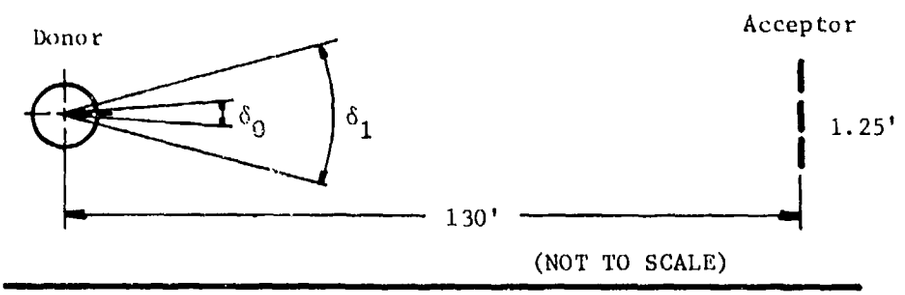

Fig. A-1 Fragment divergence angle.

The ratio of the target area to the total area which will be affected by fragmentation at a distance of 130 ft is

$$\frac{e^2}{4\pi e^2} = \frac{(1.4)^2}{4\pi(130)^2} = 7.36 \times 10^{-6} \qquad \text{(A-2)}$$

If one assumes that the presence of the tunnel walls causes twice as many fragments to strike the acceptor, then the effective area ratio becomes 1.47×10^{-5}, and the effective target edge length e becomes

$$\frac{e_1^2}{4\pi(130)^2} = 1.47 \times 10^{-5} \qquad \text{(A-3)}$$

$$e_1 = \left[(4\pi)(130)^2(1.47 \times 10^{-5})\right]^{1/2}$$

$$e_1 = 1.77 \text{ ft}$$

The new divergence angle δ_1 is

$$\delta_1 = 2 \tan^{-1} \left(\frac{e_1/2}{d}\right) \qquad \text{(A-4)}$$

$$\delta_1 = 2 \tan^{-1} \left(\frac{1.77/2}{130}\right) = 0.78°$$

This means that if the fragment distribution from the donor is radially symmetric and fragments are identical, and if the presence of the walls causes twice as many fragments to strike the acceptor, then all fragments within the divergence angle of 0.78° must strike the target. Subsequent calculations assume a fragment trajectory of 0.39° off the center axis so that if fragments along this trajectory interact with the reflected shock waves and strike the target, then greater than twice as many fragments will hit the target than if no reflecting surfaces were present.

For the purposes of this feasibility demonstration, we will assume that the blast occurs at a point source 4 ft from the walls and that the fragment travels 9 ft before interaction with two blast waves reflecting from opposite walls and striking the fragment at the same time, as shown in Figure A-2. Parameters of the shock wave which travels the shortest distance before striking the fragment are subscripted with a "1." The parameters of the second shock wave to strike the fragment are subscripted with a "2."

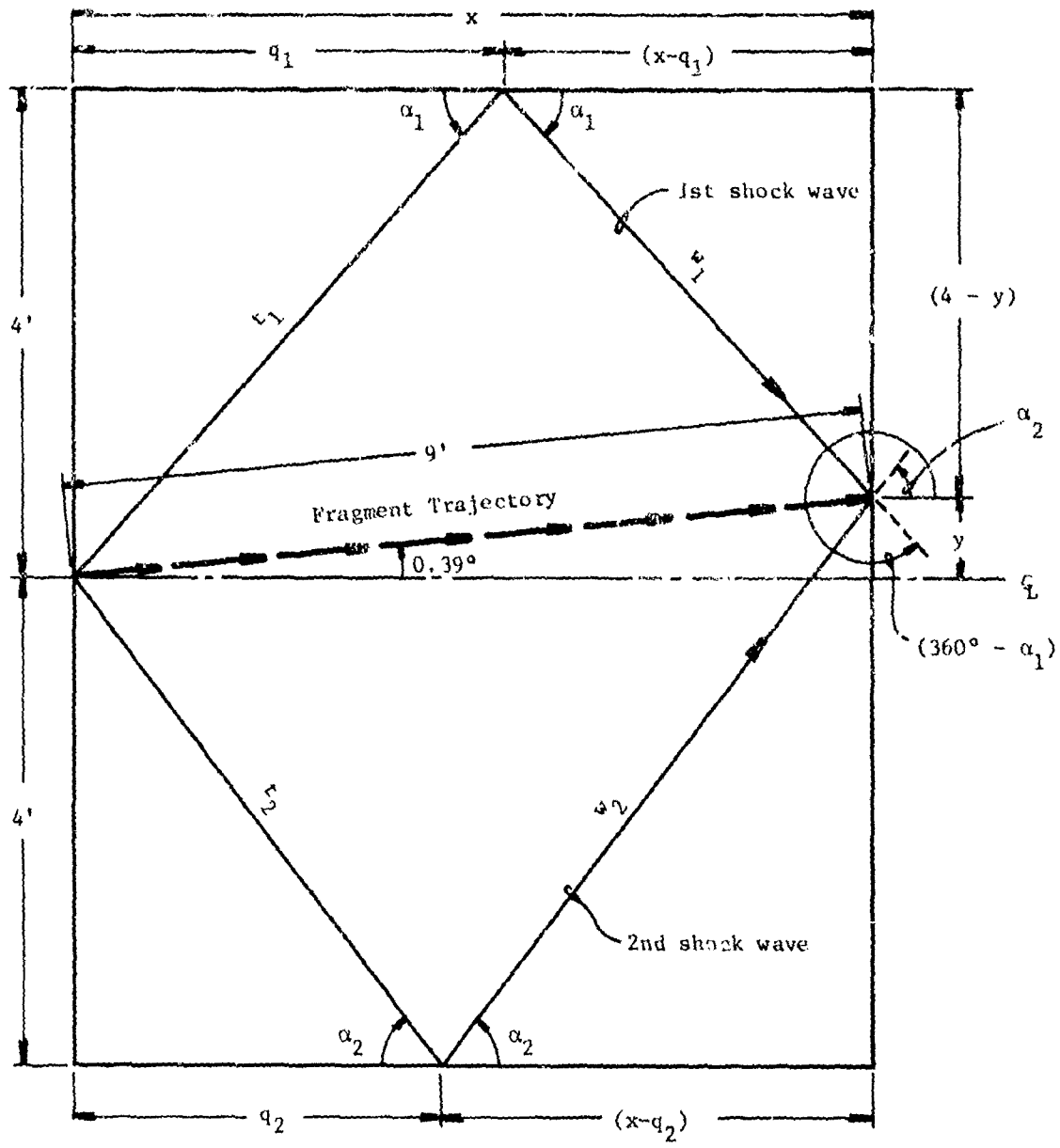

(NOT TO SCALE)

Fig. A-2 Interaction of fragment with two shock waves reflected from opposite walls.

To determine the effect of the shock waves on the fragment, it is necessary to determine the strength and direction of each shock wave. For the first shock wave, the length (t_1), which is the distance from the source of the blast to the reflecting point and the wall measured in feet, and w_1, which is the distance from the reflecting point in the wall to the interaction with the fragment measured in feet, will be calculated, and pressure and impulse will be determined from the data reported in Reference A-1.* The direction of the shock wave will be found by solving for angle α_1.

Solving for x and y, we have

$$x = 9 \cos (0.39°) \tag{A-5}$$

and

$$y = 9 \sin (0.39°) \tag{A-6}$$

where x is the projection of the fragment trajectory along the axis of the tunnel measured in feet, and y is the distance the fragment is located off the center axis of the tunnel, measured in feet.

From the first shock wave,

$$\tan \alpha_1 = \frac{4}{q_1} = \frac{4 - y}{x - q_1} \tag{A-7}$$

Solving for q_1, one can obtain

$$q_1 = \frac{\left[\dfrac{36 \cos (0.39°)}{4 - 9 \sin (0.39°)}\right]}{\left[1 + \left[\dfrac{4}{4 - 9 \sin (0.39°)}\right]\right]} \tag{A-8}$$

where q_1 is the longitudinal distance from the source of the blast to the position of the reflection of the first shock wave measured in feet.

Distances t_1 and w_1 become

$$t_1 = \sqrt{4^2 + q_1^2} = \sqrt{16 + \left\{\frac{\dfrac{36 \cos (0.39°)}{4 - 9 \sin (0.39°)}}{1 + \dfrac{4}{[4 - 9 \sin (0.39°)]}}\right\}^2}$$

$$= 6.0467 \text{ ft} \tag{A-9}$$

---

*(A-1) W. E. Baker, Explosions in Air, University of Texas Press, Austin, Texas, May 1973, pp. 150-163.

and

$$w_1 = \sqrt{(x - q_1)^2 + (4 - y)^2}$$

$$= \sqrt{\left\{9 \cos (0.39°) - \frac{\left[\frac{36 \cos (0.39°)}{4 - 9 \sin (0.39°)}\right]}{1 + \frac{4}{[4 - 9 \sin (0.39°)]}}\right\}^2 + [4 - 9 \sin (0.39°)]^2}$$

$$w_1 = 5.9541 \text{ ft} \tag{A-10}$$

Summing t_1 and w_1, one has

$$t_1 + w_1 = 12.0008 \text{ ft}$$

If the donor is 168 lb of A-7, with energy of 3.61×10^9 in-lb$_f$, scaled distance for the first shock $\bar{R}_1$ becomes, from Reference A-1,

$$\bar{R}_1 = \frac{R\, p_o^{1/3}}{E^{1/3}} \simeq 0.230 \tag{A-11}$$

where p_o is atmospheric pressure of 14.7 psi. Using Reference A-1, incident pressure p_{s_1}, impulse I_{s_1}, and the nondimensional time constant b_1 are found to be 223 psi, 0.123 psi-sec, and 27.7, respectively.

For the second shock,

$$\tan \alpha_2 = \frac{4 + y}{x - q_2} = \frac{4}{q_2} \tag{A-12}$$

where

$$q_2 = \frac{\left[\frac{36 \cos (0.39°)}{4 + 9 \sin (0.39°)}\right]}{1 + \frac{4}{[4 + 9 \sin (0.39°)]}} \tag{A-13}$$

Distances t_2 and w_2 become:

$$t_2 = \sqrt{4^2 + q_2^2} = \sqrt{16 + \left\{ \frac{\frac{36 \cos (0.39°)}{4 + 9 \sin (0.39°)}}{\left[1 + \frac{4}{4 + 9 \sin (0.39°)}\right]} \right\}^2} = 5.9952 \text{ ft} \qquad \text{(A-14)}$$

and

$$w_2 = \sqrt{(x - q)^2 + (4 + y)^2}$$

$$= \sqrt{\left\{ 9 \cos (0.39°) - \frac{\left[\frac{36 \cos (0.39°)}{4 + 9 \sin (0.39°)}\right]}{\left[1 + \frac{4}{[4 + 9 \sin(0.39°)]}\right]} \right\}^2 + [4 + 9 \sin (0.39°)]^2}$$

$$w_2 = 6.0870 \text{ ft} \qquad \text{(A-15)}$$

Summing t_2 and w_2, one has

$$t_2 + w_2 = 12.0822 \text{ ft}$$

Scaled distance for the second shock $\bar{R}_2$ becomes 0.232, and incident pressure p_{s_2}, impulse I_{s_2}, and nondimensional time constant b_2 are found to be 216 psi, 0.122 psi-sec, and 27.8, respectively, from Reference A-1. The average blast path length is approximately 12 ft, which implies a shock wave arrival time in this instance of 1.4 milliseconds. From this, one can calculate what the average fragment velocity should be in order for that fragment to interact with the converging shock waves at a point 9 ft from the source. This average velocity is 6220 ft/sec.

Figure A-3 shows the range of new flight paths the fragment must follow to be on a collision course with the acceptor after it interacts with the two reflected shock waves as demonstrated in Figure 2. The new fragment angular vector direction θ must be such that $\psi < \theta < \gamma$ in order for it to hit the acceptor. Solving for the various distances, shown in Figure A-3,

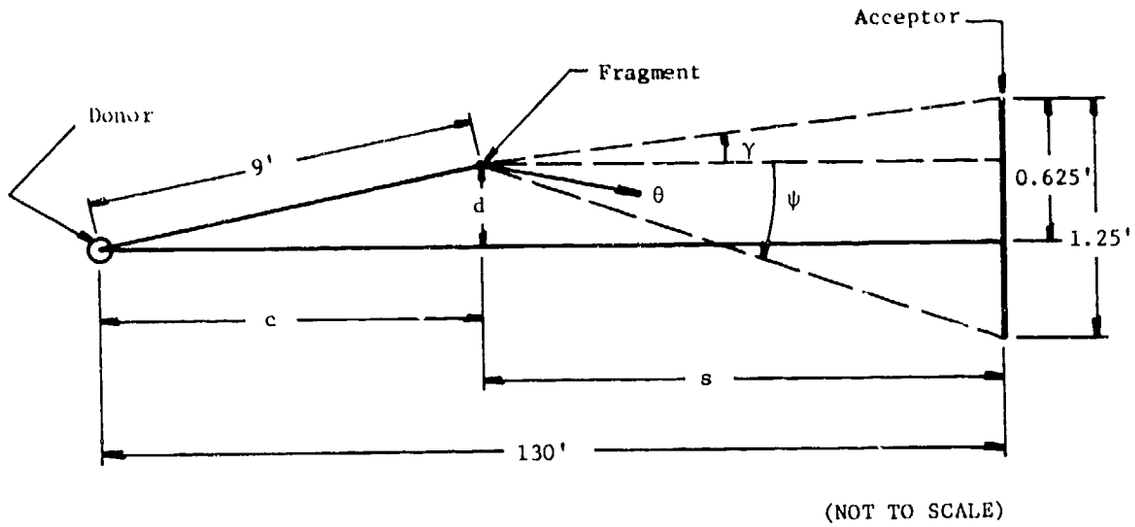

(NOT TO SCALE)

Fig. A-3 New fragment flight path for collision with acceptor.

$$c = 9 \cos (0.39°) \tag{A-16}$$

$$d = 9 \sin (0.39°) \tag{A-17}$$

$$s = 130\text{-}C = 130 - 9 \cos (0.39°) \tag{A-18}$$

Solving for angles γ and ψ, one has

$$\gamma = \text{arc tan} \left(\frac{0.625 - d}{s} \right) \tag{A-19}$$

or

$$\gamma = \text{arc tan} \left\{ \frac{[0.625 - 9 \sin (0.39°)]}{[130 - 9 \cos (0.39°)]} \right\}$$

$$\gamma = \underline{\underline{+ 0.27°}}$$

$$\psi = \text{arc tan} \left[- \left(\frac{d + 0.625}{s} \right) \right] \tag{A-20}$$

or

$$\psi = \text{arc tan} \left\{ \frac{-[9 \sin (0.39°) + 0.625]}{[130 - 9 \cos (0.39°)]} \right\}$$

$$\psi = \underline{\underline{-0.32°}}$$

That is, the new fragment trajectory θ should be such that $(-0.32°) < \theta < (+0.27°)$.

The final fragment velocity is the sum of the three vectors:

$$\vec{v}_{final} = \vec{v}_{frag} + \vec{v}_1 + \vec{v}_2 \qquad \text{(A-21)}$$

where

$\vec{v}_{frag}$ = velocity of the fragment at time of interaction with the blast waves

$\vec{v}_1$ = velocity of the fragment due to interaction with the first reflected shock wave

$\vec{v}_2$ = velocity of the fragment due to interaction with the second reflected shock wave

The initial velocity of the fragment at the time of interaction with the blast waves is

$$\vec{v}_{frag} = v_x \hat{i} + v_y \hat{j} \qquad \text{(A-22)}$$

$$\vec{v}_{frag} = v \cos (0.39°) \hat{i} + v \sin (0.39°) \hat{j} \qquad \text{(A-23)}$$

$$\vec{v}_{frag} = 6220 \cos (0.39°) \hat{i} + 6220 \sin (0.39°) \hat{j} \qquad \text{(A-24)}$$

The velocity components of the fragment due to interaction with the first reflected shock wave are

$$\vec{v}_1 = v_x \hat{i} + v_y \hat{j} \qquad \text{(A-25)}$$

$$\vec{v}_1 = v_1 \cos (360° - \alpha_1) \hat{i} + v_1 \sin (360° - \alpha_1) \hat{j} \qquad \text{(A-26)}$$

where

$$\alpha_1 = \arctan\left(\frac{4}{t_1}\right) = \arctan\left(\frac{4}{6.0467}\right)$$

$$\vec{v}_1 = v_1 \cos\left[360° - \arctan\left(\frac{4}{6.0467}\right)\right]\hat{i} + v_1 \sin\left[360° - \arctan\left(\frac{4}{6.0467}\right)\right]\hat{j} \quad \text{(A-27)}$$

The velocity components of the fragment due to interaction with the second reflected shock wave are:

$$\vec{v}_2 = v_x\hat{i} + v_y\hat{j} \quad \text{(A-28)}$$

$$\vec{v}_2 = v_s \cos(\alpha_2)\,\hat{i} + v_2 \sin(\alpha_2)\,\hat{j} \quad \text{(A-29)}$$

where

$$\alpha_2 = \arctan\left(\frac{4}{t_2}\right) = \arctan\left(\frac{4}{5.9952}\right)$$

$$\vec{v}_2 = v_2 \cos\left[\arctan\left(\frac{4}{5.9952}\right)\right]\hat{i} + v_2 \sin\left[\arctan\left(\frac{4}{5.9952}\right)\right]\hat{j} \quad \text{(A-30)}$$

Adding Eqs. (24), (27), and (30), one can obtain

$$\vec{v}_{final} = \left\{6220 \cos(0.39°) + v_1 \cos\left[-\arctan\left(\frac{4}{6.0467}\right)\right] + v_2 \cos\left[\arctan\left(\frac{4}{5.9952}\right)\right]\right\}\hat{i} + \left\{6220 \sin(0.39°) + v_1 \sin\left[-\arctan\left(\frac{4}{6.0467}\right)\right] + v_2 \sin\left[\arctan\left(\frac{4}{5.9952}\right)\right]\right\}\hat{j} \quad \text{(A-31)}$$

The new trajectory angle θ of the fragment is

$$\theta = \arctan \left\{ \frac{\left[\left(v_{final}\right)_y\right]}{\left[\left(v_{final}\right)_x\right]} \right\} \qquad \text{(A-32)}$$

Baker, et al., have developed a computer program to calculate the velocity attained by fragments subjected to blast waves, as reported in Reference A-2.* This program was recently adapted to a Hewlett-Packard 9830 minicomputer, and a copy of the program and sample output appears in Figure A-4. Pertinent parameters of this program are:

M = total mass of fragment (lb)

H = minimum transverse dimension of the mean presented area of fragment (in.)

X = dimension from front of fragment to location of its largest cross-sectional area (in.)

A = mean presented area of fragment (in^2)

C = drag coefficient of fragment

P = peak incident overpressure of blast source at point of interaction (psi)

I = peak incident specific impulse of blast source at point of interaction (psi-sec)

B = nondimensional time constant

V8 = nondimensional final velocity of fragment

V9 = final velocity of fragment (ft/sec)

Pertinent parameters from actual fragments recovered from the steel tunnel test program are shown in Table A-1.

*(A-2) W. E. Baker, J. J. Kulesz, R. E. Ricker, R. L. Bessey, P. S. Westine, V. B. Parr, and G. A. Oldham, Workbook for Predicting Pressure Wave and Fragment Effects of Exploding Propellant Tanks and Gas Storage Vessels, prepared for National Aeronautics and Space Administration by Southwest Research Institute, NASA CR-134906, 1975, Chapter 4, pp. 38-50.

```
10 REM DETERMINATION OF EFFECT OF REFLECTED BLAST WAVE ON FRAG TRAJECTORY
20 PRINT "FRAG NO    P(PSI)    I(PSI)    B(-)    V8(-)  V9(FT/S)"
30 DISP "FRAG NO =";
40 INPUT F
50 DISP "M(LBS) = ";
60 INPUT M
70 DISP "H(IN) = ";
80 INPUT H
90 DISP "X(IN) = ";
100 INPUT X
110 DISP "A(SQ IN) = ";
120 INPUT A
130 DISP "DRAG = ";
140 INPUT C
150 DISP "P(PSI) = ";
160 INPUT P
170 DISP "I(PSI-SEC) = ";
180 INPUT I
190 DISP "B = ";
200 INPUT B
210 T=2*H+X
220 W=I/((P)*(B-1+EXP(-B)))
230 Z=T/((B↑2*W)*SQR(13200↑2+(6*P*13200↑2)/(7*14.7)))
240 Y=5*P↑2/(2*14.7*(7+P/14.7))
250 S=2*P+3*P↑2/(4*14.7)
260 V=13200/T
270 U=SQR(1+6*P/(7*14.7))
280 R=(1/U-(C*X*Y*(1-Z)↑2*EXP(-B*Z)/(U*T*S)))/(1-(C*Y*(1-Z)↑2*EXP(-B*Z)/S))
290 Z1=0.5*S*R/14.7
300 Z2=C*2*Y*W*V*EXP(-B)/(B*14.7)
310 Z3=C*Y*V*B*W*EXP(-B*Z)*(2*Z-2*Z/B-Z↑2+2/B-2/B↑2-1)/14.7
320 Z4=0.5*C*Y*(1-Z)↑2*EXP(-B*Z)*R/14.7+1/U
330 V8=Z1-Z2-Z3-Z4
340 V9=V8*14.7*A*T*32.2/(M*13200)
350 WRITE (15,380)F,P,I,B,V8,V9
360 FORMAT 2X,F5.0,2F10.3,3F10.2
370 GOTO 30
380 END
```

Sample Output:

FRAG NO	P(PSI)	I(PSI)	B(-)	V8(-)	V9(FT/S)	
1	223.000	0.123	27.70	232.06	854.77	v_1
1	216.000	0.122	27.80	227.28	837.14	v_2
2	223.000	0.123	27.70	137.40	607.68	v_1
2	216.000	0.122	27.80	134.33	594.07	v_2
3	223.000	0.123	27.70	248.82	944.71	v_1
3	216.000	0.122	27.80	243.73	925.41	v_2
4	223.000	0.123	27.70	748.75	726.60	v_1
4	216.000	0.122	27.80	734.61	712.88	v_2

Fig. A-4 Computer program for calculating the velocity of fragments subjected to blast waves

Table A-1

Parameters from fragments recovered from tests

Fragment No.	Mass M (lb)	Fragment Area A (in^2)	Drag Coefficient C	Fragment Transverse Dimension H (in.)	Fragment Longitudinal Dimension X (in.)
1	7.36×10^{-3}	0.56	1.6	0.66	0.03
2	3.96×10^{-2}	2.035	1.6	1.10	0.20
3	4.25×10^{-3}	0.36	1.6	0.55	0.15
4	4.85×10^{-4}	0.0525	1.0	0.10	0.05

After the computer programs described and given in Figure A-4 for these fragments had been exercised, the velocity v_1 of each fragment due to the first shock was calculated. Similarly, the velocity $\vec{v}_2$ of each fragment due to the second shock was also calculated.

Summing $\vec{v}_1$ and $\vec{v}_2$ and the initial fragment velocity $\vec{v}_{frag}$, using Eq. (A-31), one obtains the vertical velocity component v_y and the horizontal velocity component v_x for the final fragment velocity. Using these values and Eq. (A-32), one can obtain the new fragment trajectory caused by the interaction of the fragment with the blast waves. The results of these calculations are given in Table A-2.

Table A-2

Final fragment parameters

Fragment No.	v_x (ft/sec)	v_y (ft/sec)	θ (degrees)	Remarks
1	7629	35.32	+0.27	Hit
2	7221	36.79	+0.29	No Hit
3	7778	34.73	+0.26	Hit
4	7419	37.12	+0.29	No Hit

Note from the results given in Table A-2 that the horizontal component of the velocity is greater than the initial velocity, indicating velocity enhancement by the focusing of the blast waves due to the tunnel interaction. Also, note that some of the trajectories have been altered from a no hit

$\left(\frac{\delta_1}{2} = 0.39°\right)$ to a hit trajectory of $(-0.32°) < \theta < (+0.27)$. This was the case for Fragments 1 and 3.

This analysis demonstrates that blast focusing can affect the trajectory of the fragments, and it is also possible to increase the flight velocity when reflective surfaces are present. Therefore, this explains why the tunnel confinement had an effect on increasing safe separation distance.

DISTRIBUTION LIST

		Copy No.
Commander		
US Army Armament Research and Development Command		
ATTN:	DRDAR-CG	1
	DRDAR-LC	2
	DRDAR-LCM	3
	DRDAR-LCM-S	4-15
	DRDAR-LCP-F	16
	DRDAR-TSS	17-21
Dover, NJ 07801		
Commander		
US Army Materiel Development and Readiness Command		
ATTN:	DRCDE	22
	DRCIS-E	23
	DRCPA-E	24
	DRCPP-I	25
	DRLDC	26
	DRCSG-S	27
5001 Eisenhower Avenue		
Alexandria, VA 22333		
Commander		
USDRC Installations & Services Agency		
ATTN:	DRCIS-RI-IU	28
	DRCIS-RI-IC	29
Rock Island, IL 61201		
Commander		
US Army Armament Materiel and Readiness Command		
ATTN:	DRSAR-IMB-C	30-31
	DRSAR-RD	32
	DRSAR-ISE	33-34
	DRSAR-SC	35
	DRSAR-EN	36
	DRSAR-PPW	37
	DRSAR-ASF	38-39
Rock Island, IL 61201		

Project Manager for Munition Production
Base Modernization and Expansion
US Army Materiel Development and
Readiness Command
ATTN: DRCPM-PBM-EC 40
DRCPM-PBM-T-EV 41
Dover, NJ 07801

Department of the Army
Office, Chief of Research, Development
and Acquisition
ATTN: DAMA-CSM-P 43
Washington, DC 20310

Department of the Army
ATTN: DAEN-ZCE 43
Washington, DC 20310

Commander
Chemical System Laboratory
ARRADCOM
ATTN: DRDAR-CLM-T 44
Aberdeen Proving Ground, MD 21010

Defense Contract Administration Services
1610 S. Federal Building
100 Liberty Avenue
Pittsburgh, PA 15222 45-46

Defense Documentation Center
Cameron Station
Alexandria, VA 22314 47-48

Commander
US Army Construction Engineering
Research Laboratory
ATTN: CERL-ER 59
Champaign, IL 61820

Office, Chief of Engineers
ATTN: DAEN-MCZ-E 60-61
Washington, DC 20314

DISTRIBUTION LIST

		Copy No.
Commander		
US Army Armament Research and Development Command		
ATTN:	DRDAR-CG	1
	DRDAR-LC	2
	DRDAR-LCM	3
	DRDAR-LCM-S	4-15
	DRDAR-LCP-F	16
	DRDAR-TSS	17-21
Dover, NJ 07801		
Commander		
US Army Materiel Development and Readiness Command		
ATTN:	DRCDE	22
	DRCIS-E	23
	DRCPA-E	24
	DRCPP-I	25
	DRLDC	26
	DRCSG-S	27
5001 Eisenhower Avenue		
Alexandria, VA 22333		
Commander		
USDRC Installations & Services Agency		
ATTN:	DRCIS-RI-IU	28
	DRCIS-RI-IC	29
Rock Island, IL 61201		
Commander		
US Army Armament Materiel and Readiness Command		
ATTN:	DRSAR-IMB-C	30-31
	DRSAR-RD	32
	DRSAR-ISE	33-34
	DRSAR-SC	35
	DRSAR-EN	36
	DRSAR-PPW	37
	DRSAR-ASF	38-39
Rock Island, IL 61201		

Project Manager for Munition Production
Base Modernization and Expansion
US Army Materiel Development and
Readiness Command
ATTN: DRCPM-PBM-EC 40
DRCPM-PBM-T-EV 41
Dover, NJ 07801

Department of the Army
Office, Chief of Research, Development
and Acquisition
ATTN: DAMA-CSM-P 43
Washington, DC 20310

Department of the Army
ATTN: DAEN-ZCE 43
Washington, DC 20310

Commander
Chemical System Laboratory
ARRADCOM
ATTN: DRDAR-CLM-T 44
Aberdeen Proving Ground, MD 21010

Defense Contract Administration Services
1610 S. Federal Building
100 Liberty Avenue
Pittsburgh, PA 15222 45-46

Defense Documentation Center
Cameron Station
Alexandria, VA 22314 47-48

Commander
US Army Construction Engineering
Research Laboratory
ATTN: CERL-ER 59
Champaign, IL 61820

Office, Chief of Engineers
ATTN: DAEN-MCZ-E 60-61
Washington, DC 20314

US Army Engineer District, New York
ATTN: Construction District — 62
26 Federal Plaza
New York, NY

US Army Engineer District, Baltimore
ATTN: Construction Division — 63
P.O. Box 1715
Baltimore, MD 21203

US Army Engineer District, Norfolk
ATTN: Construction Division — 64
803 Front Street
Norfolk, VA 23510

US Army Engineer District, Mobile
ATTN: Construction Division — 65
P.O. Box 2288
Mobile, AL 36628

US Army Engineer District, Fort Worth
ATTN: Construction Division — 66
P.O. Box 17300
Fort Worth, TX 76102

US Army Engineer District, Omaha
ATTN: Construction Division — 67
6014 USPO and Courthouse
215 North 17th Street
Omaha, NE 68102

US Army Engineer District, Kansas City
ATTN: Construction Division — 68-69
700 Federal Building
Kansas City, MO 64106

US Army Engineer District, Sacramento
ATTN: Construction Division — 70
650 Capitol Mall
Sacramento, CA 95814

US Army Engineer District, Huntsville
ATTN: Construction Division
P.O. Box 1600 West Station
Huntsville, AL 35807 — 71

Commander
US Army Environmental Hygiene Agency
ATTN: HSE-E
Aberdeen Proving Ground, MD 21010 — 72-73

Commander
Indiana Army Ammunition Plant
ATTN: SARIN-OR
Charlestown, IN 47111 — 74

Commander
Naval Weapons Support Center
ATTN: Code 5042, Mr. C.W. Gilliam
Crane, IN 47522 — 75

Commander
Kansas Army Ammunition Plant
ATTN: SARKA-CE
Parsons, KS 67537 — 76

Commander
Lone Star Army Ammunition Plant
ATTN: SARLS-IE
Texarkana, TX 57701 — 77

Commander
Milan Army Ammunition Plant
ATTN: SARMI-S
Milan, TN 38358 — 78

Commander
Radford Army Ammunition Plant
ATTN: SARRA-IE
Radford, VA 24141 — 79

Army Logistics Management Center
Environmental Management
ATTN: Mr. Otto Nauman
Fort Lee, VA 23801 — 80-81

Project Manager for Chemical Demilitarization
and Installation Restoration
ATTN: DRCPM-DRR, Mr. Harry Sholk 82
Aberdeen Proving Ground, MD 21010

Department of the Army
ATTN: DAEN-FEU 83
Washington, DC 20314